p.58

FINAL REPORT

THE INTERPRETATION OF CRUSTAL DYNAMICS DATA IN TERMS OF PLATE INTERACTIONS AND ACTIVE TECTONICS OF THE "ANATOLIAN PLATE" AND SURROUNDING REGIONS IN THE MIDDLE EAST

NASA GRANT NAG 5-753

PRINCIPAL INVESTIGATOR: M. Nafi Toksoz
Professor of Geophysics
Dept. of Earth, Atmospheric, and Planetary Sci.
Massachusetts Institute of Technology
Cambridge, MA 02142
(617)253-7852

CO-INVESTIGATOR: Robert Reilinger
Principal Research Scientist
Dept. of Earth, Atmospheric, and Planetary Sci.
Massachusetts Institute of Technology
Cambridge, MA 02142
(617)253-7860

DATE: 1 May, 1992

INTRODUCTION

Previous Technical Reports covered the period up to 14 October, 1991. In this Final Report, we summarize the principle accomplishments of this project. Appendix 1 is a paper submitted for publication in the Special AGU Monograph on results from the NASA CDP Program. The research described in this report is supported in part by NSF and NASA/LAGEOS II.

SUMMARY

The long-term goal of this project is to undertake a detailed study of the consequences of the Arabian plate convergence against Eurasia and its effects on the tectonics of Anatolia and surrounding regions of the eastern Mediterranean. A primary source of information is time rates of change of baseline lengths and relative heights determined by repeated SLR measurements (Sellers and Rands, 1990; Nooman et al., 1990; Ellmer et al., 1990). These SLR observations are augmented by a network of GPS stations in Anatolia, Aegea, and Greece, established and twice surveyed since 1988. The existing SLR and GPS networks provide the spatial resolution necessary to reveal the details of ongoing tectonic processes in this area of continental collision. Our effort has involved examining the state of stress in the lithosphere and relative plate motions as revealed by these space-based geodetic measurements, seismicity, and earthquake mechanisms as well as the aseismic deformations of the plates from conventional geodetic data and geological evidence. These observations are used to constrain theoretical calculations of the relative effects of: (1) the push of the Arabian plate; (2) high topography of Eastern Anatolia (~2000 m); (3) the geometry and properties of the African-Eurasian plate boundary; (4) subduction under the Hellenic Arc and southwestern Turkey; and (5) internal deformation and rotation of the Anatolian plate.

ACCOMPLISHMENTS

Our principal efforts have been directed along the following lines: (1) Continuing analysis of seismicity and earthquake focal mechanisms; (2) Expanding our finite element models to include the entire Anatolian plate, the Aegean Sea and the Northeastern Mediterranean Sea, northwest Iran and the Caucasus; (3) Investigating the tectonic processes associated with ongoing continental collision in eastern Anatolia using neo-tectonic and geophysical information; and (4) Initiating an international program to densify SLR coverage in the eastern Mediterranean with GPS (our participation in this effort has been partly supported by NSF and NASA Lageos II). These efforts, described below, are designed to provide an improved basis for interpreting NASA's SLR measurements in this region.

Seismicity, Earthquake Source Mechanisms, and Conventional Geodetic Observations

The seismicity of the Middle East and that of Turkey are shown in Figures 2 and 4, respectively. Epicenters generally outline the major fault zones shown in Figures 1 and 3. However, there are a significant number of earthquakes occurring away from these "plate boundaries", indicating the presence of smaller faults and deformations in the plate interiors.

Earthquake source mechanisms (Toksoz et al., 1977; McKenzie, 1978; Buyukasikoglu, 1979, 1980; Kocaefe and Ataman, 1982; Rotstein and Kafka, 1982; Jackson and McKenzie, 1984; Lyberis, 1984; Eyidogan and Jackson, 1985; Alptekin et al., 1986; England and Jackson, 1990) shown in Figure 5 define the relative motions across the faults and provide information on prevailing stress directions. The fault mechanisms are consistent with "tensions" in the Aegean region. This indicates a major change in the state of stress in the Anatolian plate. We are continuing to compile and re-analyze earthquake mechanisms as well as the geologic evidence in central Anatolia to determine where and how the stress regime changes. Mechanisms for extension in Aegea are being coupled with other mechanisms to explain this change in the state of stress. One possibility to be taken into account is the rotation of the Anatolian plate. Paleomagnetic data from Central Anatolia (Sanver and Ponat, 1981) show that the Anatolian plate has rotated counter clockwise by about 15° in the past 45 million years. Such a rotation, coupled with a possible anchoring due to subduction could contribute to the tensile regime of Western Anatolia. Westaway (1990) shows evidence for the rotation of individual blocks in western Turkey. These models are being incorporated as constraints in both close scrutiny of the data and theoretical modeling of plate interactions (see below).

In addition to deformations shown by earthquakes, there is ample evidence for aseismic deformation in and around the Anatolian plate. Geodetic and creep measurements on the North Anatolian fault show that there is creep on at least one segment of the fault, at a rate of about 1 cm/yr. To the west of the site, a major geodetic network shows that one branch of the fault (that broke in the 1967 earthquake) is locked, while a southern branch is deforming at a rate of 1.2 cm/year. The combination of seismic dislocations and creep gives a fault dislocation rate of about 1.2 to 2.0 cm/year across the North Anatolian Fault zone. This deformation rate is in good agreement with rates derived from our analysis of SLR and GPS observations (see below and Appendix 1). These are the first hard numbers we have on the present-day motion of the Anatolian plate and are extremely important for constraining models of contemporary plate interactions.

Finite Element Modeling

The purpose of this aspect of our research program is to develop a simple but robust approach to modeling plate interactions using a contact problem in 2-D elastic finite element method. An individual plate is considered as a continuum, whereas an aggregate of plates is treated as a discontinuum such that plate boundaries are represented as contact surfaces. The behavior of plates at the contacts is defined by the Coulomb-Navier failure criterion, and three types of contacts are considered: sliding contact (slip), tension release (separation), and sticking contact (single-node continuum). The first and second modes correspond to transcurrent and divergent plate boundaries respectively. Convergent motion at plate boundaries is achieved by the double-node differential displacement technique with a recursive solution. Preliminary models for the Eastern Mediterranean, where tectonic deformation is produced by the interactions of the Eurasian, Arabian and African plates, was carried out. Figure 6 shows the finite element grid and defined contact zones used for these preliminary models. GPS estimates of horizontal crustal motions across the North Anatolian fault and in western Turkey (see below and Appendix 1) and geological observations of fault offsets were used to constrain displacements. Figure 7 shows modeled displacements for the Eastern Mediterranean region. We find that the deformation pattern in the Eastern Mediterranean is substantially controlled by differential motion between the African and Arabian plates and southwestward migration of the Hellenic arc. We note that the southwestward migration of the Hellenic arc required to fit the GPS observations is roughly consistent in sense with initial estimates of crustal motion determined from SLR observations (Ambrosius, personal communication 1991). The larger motions of the arc suggested by these models (relative to those estimated from SLR) may reflect SLR and/or GPS measurement uncertainties and/or the influence of buoyancy forces on crustal motions in western Turkey. Additional modeling is being undertaken to determine the relative importance of buoyancy forces caused by elevation changes.

Neotectonic Studies

1. Strike-Slip Fault Geometry and Its Relationship to Earthquake Activity (Barka et al., 1987, 1988; Barka and Kadinsky-Cade, 1988).

Analysis of Turkish strike-slip faults indicates that detailed fault geometry plays an important role in controlling earthquake rupture. Empirical relationships are used to estimate possible locations and sizes of future strike-slip events. These results have implications for earthquake activity on other strike-slip faults such as the San Andreas in California.

2. Tectonic Processes of the Continental Collision in the Vicinity of the Maras Triple Junction, Southern Turkey (Barka et al., 1990)

Study of the geometry, kinematics and slip rates of the structures surrounding the Maras Triple Junction, formed by the collision between the Arabian, African and Eurasian plates in eastern Turkey, provides information on the continental collision process. Deformation is diffused over a region more than 500 km wide, from the Taurus to Caucasus Mountains within which several continental blocks escape from the maximum convergence zone. The collision initiated about 13 Ma ago and had two phases: the first caused thickening of the crust by thrusting, the second involved block escape. We estimate that 40 % of the overall shortening is taken up by block escape along strike-slip faults, and the remainder by thrusting and folding throughout the collision zone.

3. Eastern Turkey and Caucasia (Alptekin et al., 1986; Kadinsky-Cade et al., 1989)

Armenian (7 December 1988) and Iran (20 June 1990) earthquake source mechanisms provide good examples of the deformation patterns of the lesser Caucasus and the western shores of the Caspian Sea, respectively. The mechanisms (large "beach balls" in Figure 8) indicate that both earthquakes included a combination of strike-slip and thrust motions. Near the Caspian, continental crust is overriding the oceanic crust of the southern Caspian Sea. In Armenia there is both thrusting and strike-slip motion representing the eastward escape of the block, along with some thrusting. Further north on the greater Caucasus and northeastern shores of the Black Sea, earthquake mechanisms are almost purely thrust, as shown in Figure 9 (Alptekin et al., 1986). Taking into account the one thrust earthquake to the south along with the steep slope of the continental margin, it is possible that the eastern Black Sea is being overthrust by the continental crust, both from the north and the south.

4. Mapping of active faults from remote Thematic Mapper and radar imagery (Gulen et al., 1991).

While we have easy access to field sites in Turkey, access to northwest Iran and Armenia is more difficult. However, we have made considerable progress identifying active faults using space imagery (SPOT, Thematic Mapper and radar---SEASAT, SIR A, SIRB).

<u>GPS Densification of SLR Measurements in the Eastern Mediterranean</u>

The Turkey GPS experiment is part of a broader effort, involving a number of institutions, to understand better the kinematics and dynamics of on-going tectonic activity in the Eastern Mediterranean region. The tectonics of this region are dominated by collision of the Arabian and African plates with the Eurasian plate. These plate interactions give rise to active subduction along the Hellenic arc, back-arc spreading in the Aegean sea and the Aegean trough region of S.W. Turkey, continent-continent collision and associated mountain building in the Caucasus-Bitlis Zagros ranges of eastern Turkey and adjacent areas, continental escape and major block rotation of the Anatolian and East Anatolian micro-plates with associated strike-slip faulting (including the North Anatolian fault), and strike-slip faulting along the Dead Sea transform. Virtually all types of continental deformation occur within the borders of Turkey.

The MIT group, with support from UNAVCO and in collaboration with Hacettepe University, initiated GPS measurements in Turkey in 1988 with the establishment of 14 sites primarily in western and central Turkey. During this campaign, GPS measurements were also made by our group at the 4 mobile SLR stations established in Turkey by WEGENER. In 1989, MIT/UNAVCO, in collaboration with the Turkish Union of Geodesy and Geophysics (TUJJB), established 18 GPS sites primarily in the continental collision-escape zone of eastern Turkey. Independent, but closely coordinated GPS campaigns were carried out simultaneously by IFAG/TUJJB, and the University of Durham/TUJJB. IFAG/TUJJB made measurements at SLR sites and established GPS "foot prints" on the scale of a few 10s of kilometers around each SLR site (~3 per SLR site). The Durham/TUJJB group observed a dense network in the Aegean trough region of western Turkey, including 5 of the sites established by our group in 1988.

During the fall of 1990, regional GPS surveys to monitor tectonic deformation were undertaken by MIT/UNAVCO, IFAG/WEGENER, and ETH-Zurich. Excellent communication and cooperation were maintained throughout the planning and execution phases of the 1990 GPS surveys. Each group worked in collaboration with the TUJJB which also served to coordinate activities between groups. IFAG/TUJJB undertook a major campaign involving 10 receivers observing for approximately 6 weeks. The campaign included two phases: the first consisting of a regional campaign to observe 22 sites in the Turkish first-order geodetic control network and a number of points along a precise leveling line in western Turkey, the second consisting of a dense survey along a 250 km segment of the North Anatolian fault in western Turkey (east end of Marmara Sea to Gerede). ETH-Zurich, in collaboration with Istanbul Technical University, established a network of sites in the Marmara Sea region (west of IFAG North Anatolian fault network) to investigate activity along the westernmost segment of the NAF where it splays into a number of active strands. Details of the IFAG and ETH-Zurich experiments can be obtained from Hermann Seeger, IFAG and H. -G. Kahle, ETH-Zurich.

Details of the M.I.T./TUJJB 1990 GPS campaign were reported in a previous annual technical report. Briefly, we reobserved 10 GPS sites in western Turkey established by our group in 1988. Simultaneous observations were carried out by IFAG at 3 SLR sites in central Turkey. In addition, reference marks on the scale of 100 m were set and surveyed at 13 sites in western Turkey. Initial estimates of horizontal crustal motions determined from the 1988-1990 GPS observations are presented and described in Appendix 1.

A first repeat of the eastern Turkey GPS network was accomplished in 1991. The principal objectives/accomplishments of the 1991 E. Turkey GPS Campaign included:

1) Reobservation of the 1989 GPS network to obtain initial estimates of deformation rates and styles in the E. Turkey continental collision zone.
2) Measurement of baselines crossing the western and central segments of the N. Anatolian fault to obtain additional information on rates of strain accumulation.
3) Establishment of new stations to define better movements across the Dead Sea fault, and N-S shortening between the Arabian and Eurasian plates.

4) Tying the E. Turkey network to the GPS network across the Caucasus established in July 1991.
5) Establishing and surveying reference marks for E. Turkey GPS stations.
6) Making initial GPS measurements at the new SLR pad in Karacadag (to replace Diyarbakir site) and tying the permanent Ankara GPS station to the Hacettepe University, Ankara site established by MIT in 1988.

The 1991 field campaign was a collaborative effort with the TUJJB and was coordinated with GPS measurements carried out by IFAG. Seven Trimble 4000 SST GPS receivers and 1 set of conventional survey equipment (for reference marks) were provided by UNAVCO for this experiment. Only 2 U.S. participants were involved in field operations (Reilinger, UNAVCO Engineer). All other participants (6 primary GPS operators, 8 assistants) were provided by TUJJB.

Figure 10 shows regional GPS sites in Turkey established by our group between 1988 and 1991.

The 1988 and 1990 GPS observations in western Turkey (see previous section) were reduced at M.I.T. jointly with our Turkish collaborators. An abstract describing our initial results was submitted for presentation at the 1991 Fall AGU Meeting (Oral et al., 1991). The GAMIT and GLOBK GPS software packages were used to analyze double difference data to estimate site coordinates, orbital elements, atmospheric parameters, earth orientation parameters, and phase ambiguities. SLR site positions have not been imposed in our initial solutions. Figure 11 shows relative horizontal site velocities assuming no motion at Yigilca, an SLR station located north of the North Anatolian fault. The assumption of stability of the Yigilca SLR station is consistent with results reported from analysis of European SLR observations (Ambrosius, personal communication, 1991). The solutions shown in Figure 11 indicate right-lateral strike slip motion across the western and central sections of the North Anatolian fault at a rate of approximately 2 $\pm$0.5 cm/yr and southwestward "escape" of western Anatolia at approximately 4 $\pm$ 1 cm/yr. These initial results represent the first quantitative estimates of present-day deformation rates in this area.

REFERENCES

Allen, C. R., 1969. Active faulting in northern Turkey, *Contrib. 1577,* 32 pp., Div. of Geol. Sci., Calif. Inst. of Technol., Pasadena.

Allen, C. R., 1975. Geological criteria for evaluating seismicity, *Bull. Geol. Soc. Am., 86,* 1041–1057.

Alptekin, O., 1973. Focal mechanism of earthquakes in western Turkey and their tectonic implications (Ph.D. thesis): Socorro, New Mexico Inst. Mining and Tech., 189 pp.

Alptekin, O., Nabelek, J.L. and Toksöz, M.N., 1986. Source mechanism of the Bartin earthquake of September 3, 1968 in northwestern Turkey: Evidence for active thrust faulting of the southern Black Sea margin, *Tectonphysics, 122,* 73–88.

Ambraseys, N.N., 1970. Some characteristic features of the North Anatolian fault zone, *Tectonophysics, 9,* 143–165.

Ambraseys, N.N., and Finkel, C.F., 1987. Seismicity of the Northeast Mediterranean Region during early 20th Century. *Annales Geophysicae, 5B* (in press).

Ambraseys, N.N., and Finkel, C.F., 1987a. The Saros-Marmara earthquake of 9 August 1912, *J. Earthquake Eng. Struct. Dyn., 15(2),* 189–211.

Angelier, J., Dumont, J.F., Karamanderesi, H., Poisson, A., Simsek, S., and Uysal S., 198l. Analysis of fault mechanisms and expansion of southwestern Anatolia since the Late Miocene, *Tectonophysics, 75,* T1–T9.

Arpat, E., and Saroglu, F., 1972. The East Anatolian fault system: thoughts on its development, *Bull. Min. Res. and Explor. Inst. of Turkey (M.T.A.), 78,* 33–39.

Arpat, E., and Saroglu, F., 1975. Some recent tectonic events in Turkey, *Türkiye Jeoloji Kurumu Bült., 18,* 91–101, (in Turkish with Engl. abstr.).

Arpat, E., F. Saroglu, and H.B. Iz, 1977. The 1976 Caldiran earthquake, *Yeryuvari Insan, 2,* 29–41.

Barka, A.A. and Gulen, L., 1988. New constraints on age and total offset of the North Anatolian fault zone: Implications for tectonics of the Eastern Mediterranean region, (In), *Melih Tokay Geology Symposium,* Spec. Publ. Middle East Tech. Uni. Ankara, Turkey, in press.

Barka, A. and Kadinsky-Cade, K., 1988. Strike-slip fault geometry in Turkey and its influence on earthquake activity, *Tectonics, 7,* 663–684.

Barka, A., Kadinsky-Cade, K., and Toksöz, M.N., 1987. North Anatolian fault geometry and earthquake activity, *Seismol. Res. Lett., 58,* 31–32.

Barka, A.A., Gulen, L. and Toksöz, M.N., 1990. Tectonic processes of the continental collision in the vicinity of the Maras triple junction, southern Turkey, *Tectonophysics,* submitted.

Barka, A., Toksöz, M.N., Kadinsky-Cade, K., and Gulen, L., 1988. The segmentation, seismicity and earthquake potential of the eastern part of the North Anatolian fault zone, *Special Publication of Hacettepe Univ.,* Ankara, Turkey, in press.

Bathe, K-J. and Chaudhry, A., 1985. A solution method for axisymmetric contact problems, *Int. J. Num. Meth. Eng., 21,* 65–88.

Bathe, K-J. and Mijailovich, S., 1987, Finite element analysis of frictional contact problems, *J. De Mechanique Theorique et Applique,* 375–389.

Bird, P., Toksöz, M.N., and Sleep, N.H., 1977. Thermal and mechanical models of the continent-continent convergence zones, *J. Geophys. Res., 80,* 4405–4416.

Buyukasikoglu, S., 1979. *Seismolojik Verilere Gore Guney Anadolu ve Dogu Akdenizde Avrasya-Africa Leuha Sinirinin Ozellikleri,* 75 pp., Istanbul Technical University, Istanbul.

Buyukasikoglu, S., 1980. Eurasian-African plate boundary in southern Turkey and eastern Mediterranean. In: *Proceedings of the 7th World Conference on Earthquake Engineering, Geoscience Aspects, Part 1. 1,* 209–212.

Canitez, N., and Ücer, B., 1967. *A Catalogue of Focal Mechanism Diagrams for Turkey and Adjoining Areas. I.T.U. Maden Fak. Arz Fiziji Enst. Yay., 25,* 111.

Caputo, M., Panza, G.F., and Postpischl, D., 1970. Deep structure of the Mediterranean Basins, *J. Geophys. Res., 75,* 4919–4923.

Chaudry, A. and Bathe, K-J., 1986. A solution method for static and dynamic analysis of three-dimensional contact problems with friction, *Comp. Struct., 24,* 885–873.

Crampin, S., and Evans, R., 1986. Neotectonics of the Marmara Sea region of Turkey, *J. Geol. Soc. London, 143,* 343–348.

Davis, G.A. and Burchfiel, B.C., 1973. Garlock Fault: An intracontinental transform structure, southern California, *Geol. Soc. Am. Bull., 84,* 1407–1422.

Dewey, J.F., Pitman, W.C., Ryan, W.F.R., and Bonnin, J., 1973. Plate tectonics and the evolution of the Alpine system. *Geol. Soc. Am. Bull., 84,* 3127–3180.

Dewey, J.F. and A.M.C. Sengör, 1979. Aegean and surrounding regions: Complex multiple and continuum tectonics in a convergent zone, *Geol. Soc. Am. Bull., 90,* 84–92.

Dewey, J.F., Hempton, M.R., Kidd, W.S.F., Saroglu, F. and Sengör, A.M.C., 1986. Shortening of continental lithosphere: the neotectonics of Eastern Anatolia—a young collision zone. In *Collision Tectonics,* eds. M.P. Coward and A.C. Ries, *Geol. Soc. Spec. Publ. 19,* London, 3–36.

Ellmer, W., Foerste, C., Reigber, C.,and Drewes, H., 1990. Present day plate motions derived by DGFI, Crustal Dynamics Principal Investigators Meeting, Maryland, October 25–26.

England, P. and Jackson, J., 1989. Active deformation in the continents, *Ann. Rev. Earth and Planetary Sci., 17,* 197–226.

England, P. and McKenzie, D., 1982. A thin viscous sheet model for continental deformation, *Geophys. J. R. astr. Soc., 70,* 295–231.

England, P. and McKenzie, D., 1983. Correction to: A thin viscous sheet model for continental deformation, *Geophys. J. R. astr. Soc., 73,* 523–532.

Eyidogan, H., and Jackson, J., 1985. A seismological study of normal faulting in the Demirci, Alasehir and Gediz earthquakes of 1969–70 in western Turkey: implications for the nature and geometry of deformation in the continental crust. *Geophys. J.R. Astr. Soc., 81,* 569–608.

Goodman, R.E. and St. John, C., 1976. Finite element analysis for discontinuous rocks, 149–175.

Gulen, L., Prange, M., and Toksöz, M.N., 1991. Fault detection using spaceborn imaging radar, submitted to AAPG.

Hall, R., 1976. Ophiolite emplacement and the evolution of the Taurus Suture Zone, southeastern Turkey, *Bull. Geol. Soc. Am., 87,* 1078–88.

Hashida, T., Stavrakakis, G., and Shimazaki, K., 1988. Three-dimensional seismic attenuation astructure beneath the Aegean region and its tectonic implications, *Tectonophysics, 145,* 43–54.

Jackson, J., and McKenzie, D.P., 1984. Active tectonics of the Alpine-Himalayan Belt between western Turkey and Pakistan, *Geophys. J.R. Astr. Soc., 77,* 185–246.

Jackson, J. and McKenzie, D., 1988. The relationship between plate motions and seismic tremors, and the rates of active deformation in the Mediterranean and Middle East. *Geophys. J. R. Astr. Soc., 93,* 45–73.

Kadinsky-Cade, K., Barka, A.A., and Toksöz, M.N., 1989. The December 7, 1988 Ms = 6.8 Armenian earthquake: Source characteristics and regional deformation, *Eos, 70,* 306.

Kasapoglu, K.E., and Toksöz, M.N., 1983. Tectonic consequences of the collision of the Arabian and Eurasian plates: finite element models, *Tectonophysics, 100,* 71–95.

Kasapoglu, K.E. and Toksöz, M.N., 1991. Plate-motion induced deformations in the Eastern Mediterranean, *Tectonophysics*, in press.

Kaya, O., 1981. Miocene reference sections for the coastal parts of West Anatolia. *Newsletter of Stratigraphy, 10,* 164–191.

Ketin, I., 1969. Über die nordanatolische Horizontalverschiebung, *Bull. Miner. Res. Explor. Inst. Turk., 72,* 1–28.

Ketin, I., and Roesli, F., 1953. Makroseismische Untersuchungen über das nordwest-anatolische Beben vom 18 März 1953. *Ecologae Geol. Helv., 46,* 187–208.

Kocaefe, S.S., and Ataman, G., 1982. Actual tectonics of Western Anatolia (in Turkish) *Yerbilimleri, 9,* 149–162.

Kumbora, K., Solutions of the contact problems by the assumed stress hybrid model, Ph.D. thesis, M.I.T., 144 PP., 1979.

LePichon, X. and Angelier, J., 1979. The Hellenic arc and trench system: a key to the Neotectonic evolution of the eastern Mediterranean arc. *Tectonophysics, 60,* 1–42.

Lybéris, N., 1984. Tectonic evolution of the north Aegean Trough, in *The Geological Evolution of Eastern Mediterranean, Spec Publ.* edited by J. G. Dixon and A. H. F. Robertson, pp. 711–725, Geological Society of London.

Makris, J., 1978. The crust and upper mantle of the Aegean region from deep seismic sounding, *Tectonophysics, 46,* 269–284.

McKenzie, D.P., 1972. Active tectonics of the Mediterranean region, *Geophys. J.R. Astr. Soc., 30(2),* 109–185.

McKenzie, D.P., 1978. Active tectonics of the Alpine-Himalayan belt: the Aegean Sea and surrounding regions (tectonics of Aegean region). *Geophys. J.R. Astr. Soc., 55,* 217–254.

Mercier, J.L., 1981. Extensional-compressional tectonics associated with the Aegean arc: comparison with the Andean Cordillera of south Peru—north Bolivia. *Philos. Trans. R. Soc. London, Ser. A 300,* 337–355.

Mercier, J.L., Sorel, D. and Simeckis, K., 1987. Changes in the state of stress in the overriding plate of a subduction zone: the Aegean arc from the Philocene to present. *Anne. Tectonicae, 1,* 20–39.

Molnar, P., and Tapponnier, P., 1975. Cenozoic tectonics of Asia: effects of a continental collision. *Science, 189,* 419–26.

Noomen, R., Ambrosius, B.A.C., and Wakker, K.F., 1990. Determination of station coordinates and motions from Lageos laser range observations, Crustal Dynamics Principal Investigators Meeting, Maryland, October 25–26.

Papazachos, B.C. and Comminakis, P.E., 1971. Geophysical and tectonic features of the Aegean arc. *J. Geophys. Res., 76,* 8517–8533.

Rigo de Righi, M. and Coretesini, A., 1964. Gravity tectonics in foothills structure belt of southeast Turkey. *Bull. Am. Assoc. Petrol. Geol., 48,* 1911–1937.

Rotstein, Y., and A.L. Kafka, 1982. Seismotectonics of the southern boundary of Anatolia, eastern Mediterranean region, subduction, collision and arc jumping, *J. Geophys. Res., 87,* 7694–7706.

Sanver, M. and Ponat, E., 1981. Paleomagnetic data and rotation of Kirsehir Masifi (in Turkish), *Yerbilimleri, 2, Nr. 3-4,* 231–238.

Sellers, P. and Randa, P.N., 1990. Crustal dynamics in Europe and the Mediterranean determined by the pseudo-short arc technique, Crustal Dynamics Principal Investigators Meeting, Maryland, October 25–26.

Sengör, A.M.C., and Kidd, W.S.F., 1979. Post-collisional tectonics of the Turkish-Iranian plateau and a comparison with Tibet, *Tectonophysics, 55,* 361–376.

Sengör, A.M.C., Gorur, N., and F. Saroglu, 1985. Strike-slip faulting and related basin formation in zones of tectonic escape: Turkey as a case study, in *Strike-slip Faulting and Basin Formation,* (Biddle, K.T. and N. Christie-Blick, eds.) Society of Econ. Paleont. Min. Sec. Pub,. 37, 1985.

Sengor, A.M.C., 1987. Cross-faults and differential stretching of hanging walls in regions of low-angle normal faulting: examples from western Turkey: In M.P. Conrad, J.F. Dewey, and P.L. Hancock (Editors) *Continental Extensional Tectonics,* Geol. Soc. London. Spec. Publ. 28, 575–589.

Seymen, I., and A. Aydin, 1972. The Bingöl earthquake fault and its relation to the North Anatolian fault zone, *Bull. Miner. Res. Explor. Inst. Turk., 79,* 1–8.

Spakman, W., Wortel, M.J.R., and Vlaar, N.J., 1988. The Hellenis subduction zone: A tomographic image and its geodynamic implications, *Geophys. Res. Lett., 15,* 60–63.

Tapponnier, P., and Molnar, P., 1977. Active faulting and Cenozoic tectonics of China. *J. Geophys. Res., 82,* 2905–30.

Toksöz, M.N., E. Arpat, and F. Saroglu, 1977. East Anatolian earthquake of 24 November 1976, *Nature, 270,* 423–425.

Toksöz, M.N., Guenette, M., Gulen, L., Keough, G., and Pulli, J.J., 1984. Source mechanism of Oct. 30, 1983 earthquake in northeastern Turkey (unpublished manuscript).

Toksöz, M.N. and Kasapoglu, E., 1988. Collision of the Arabian and Eurasian plates: Finite element models, *EOS, 69,* 331.

Toksöz, M.N., Oral. M.B., and Barka, A.A., 1989. Tectonic deformations in the eastern Mediterranean and Caucasia due to the collision of the Arabian and Eurasian plates, *Eos, 70,* 1372.

Toksöz, M.N., A.F. Shakal, and A.J. Michael, 1979. Space-time migration of earthquakes along the N. Anatolian fault zone and seismic gaps, *Pure Appl. Geophys., 117,* 1258–1270.

Wdowinski, S., O'Connell, R. and England, P., 1989. A continuum model of continental deformation above subduction zones: Application to the Andes and the Aegean, *J. Geophys. Res., 94,* 10331–10346.

Westaway, R., 1990. Block rotations in western Turkey, 1. observational evidence, *J. Geophys. R., 95,* 19857–19884.

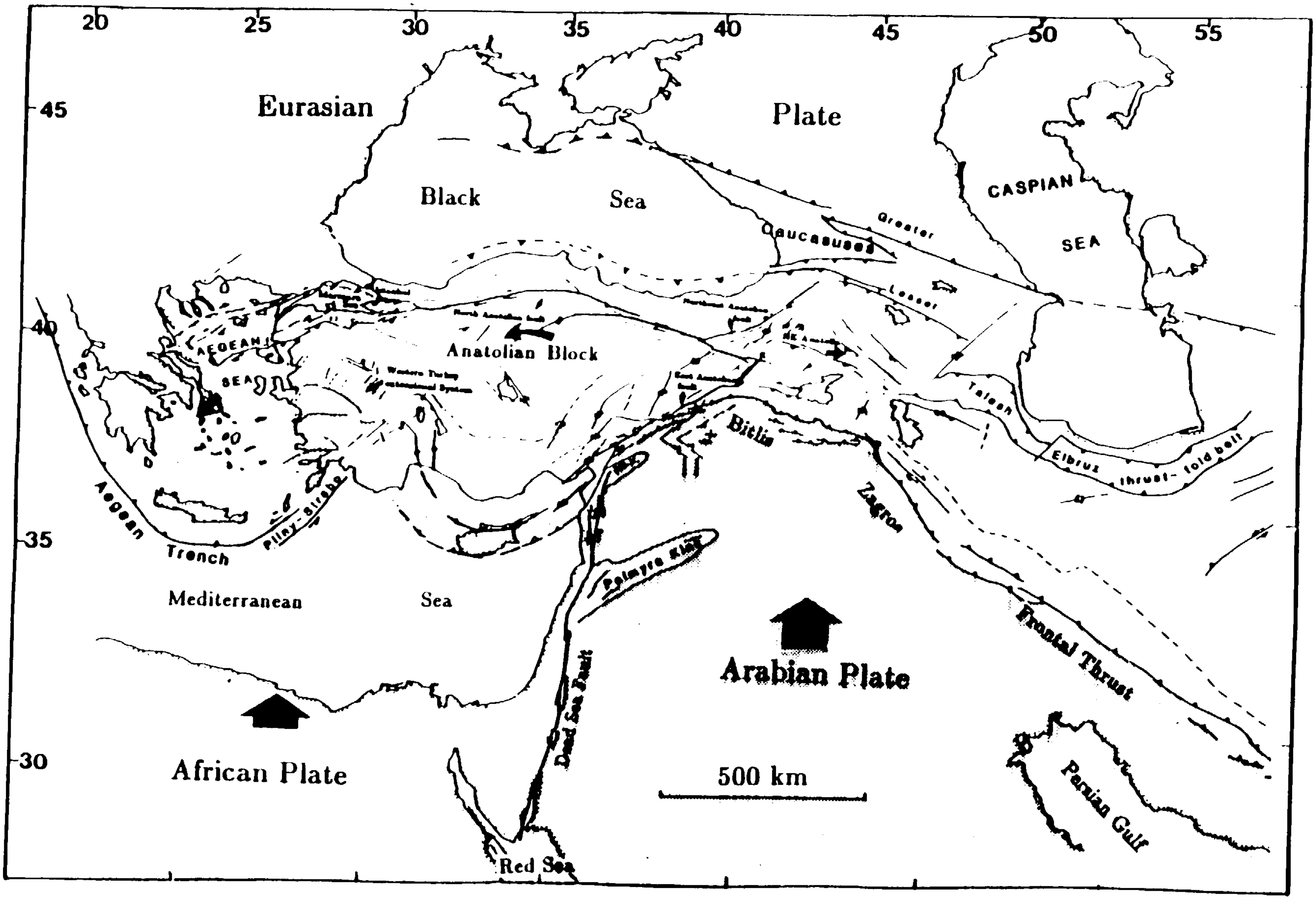

Figure 1. The major deformational units of the Aegea, eastern Mediterranean, and Middle East. Large arrows show approximate movements of the Arabian and African plates with respect to the Eurasian plate.

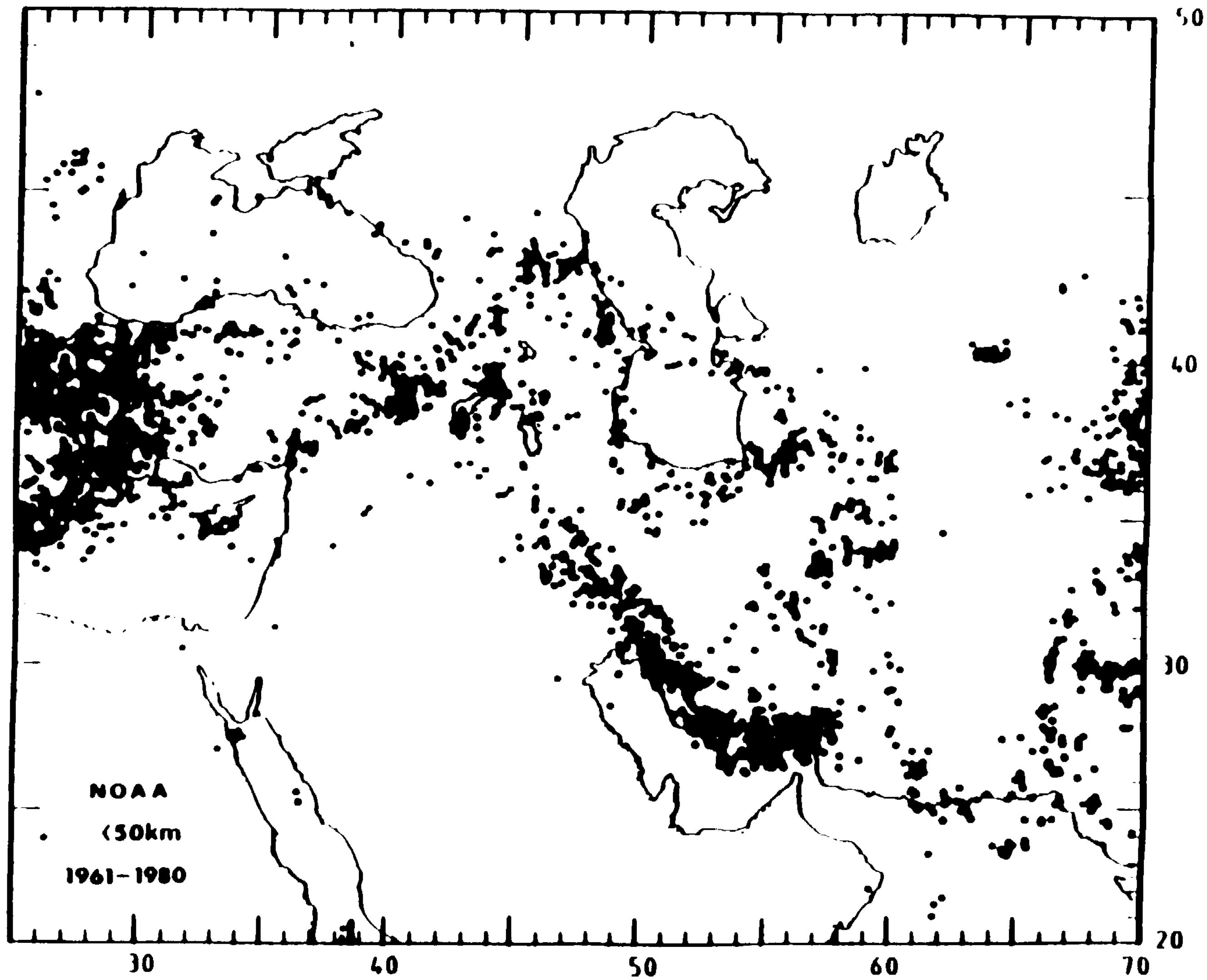

Figure 2. Distribution of earthquake epicenters shallower than 50 km in the eastern Mediterranean and Middle East for the period 1961-1980 (after Jackson and McKenzie, 1984).

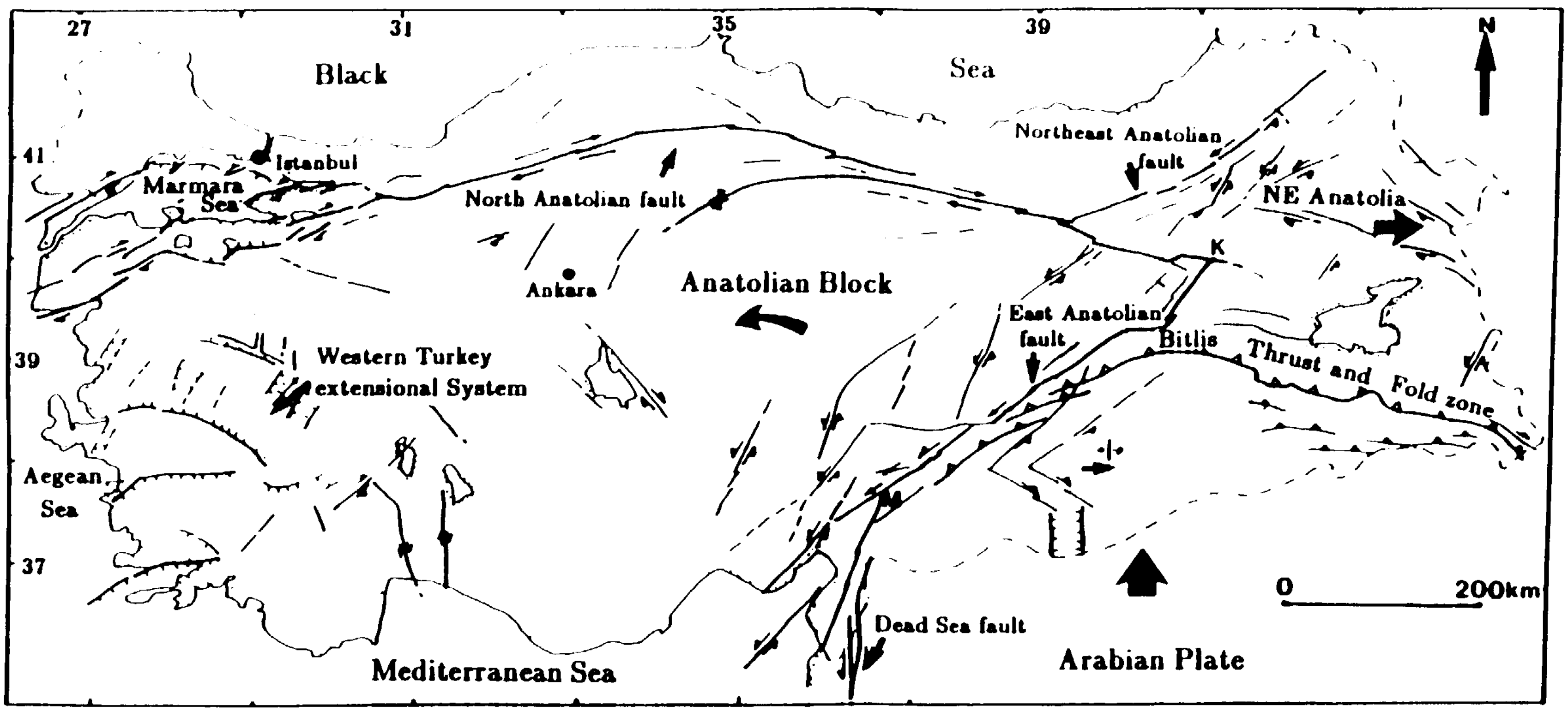

Figure 3. Major tectonic elements of Turkey (from Barka and Kadinsky-Cade, 1988).

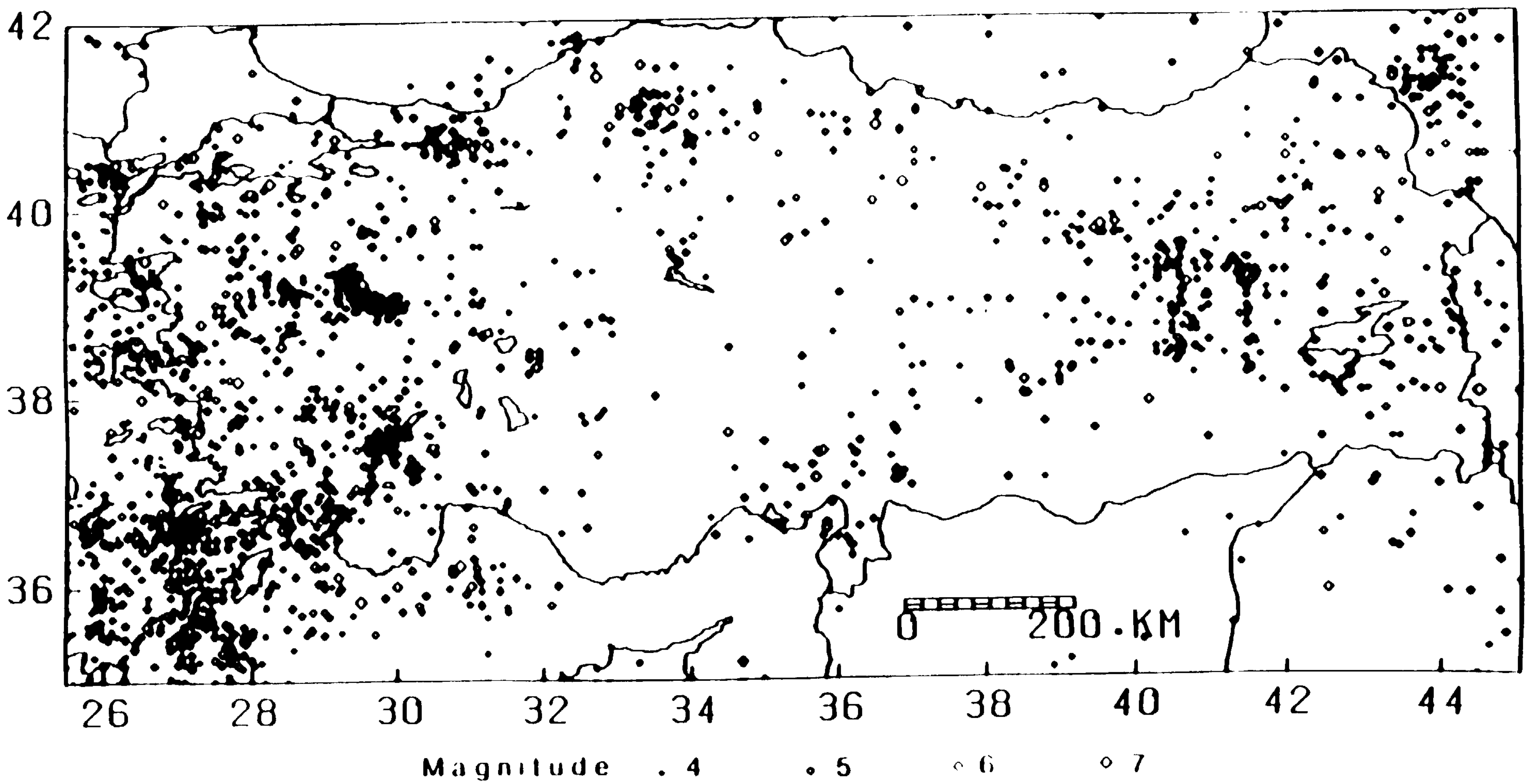

Figure 4. Distribution of earthquake epicenters in Turkey for the period 1900-1975.

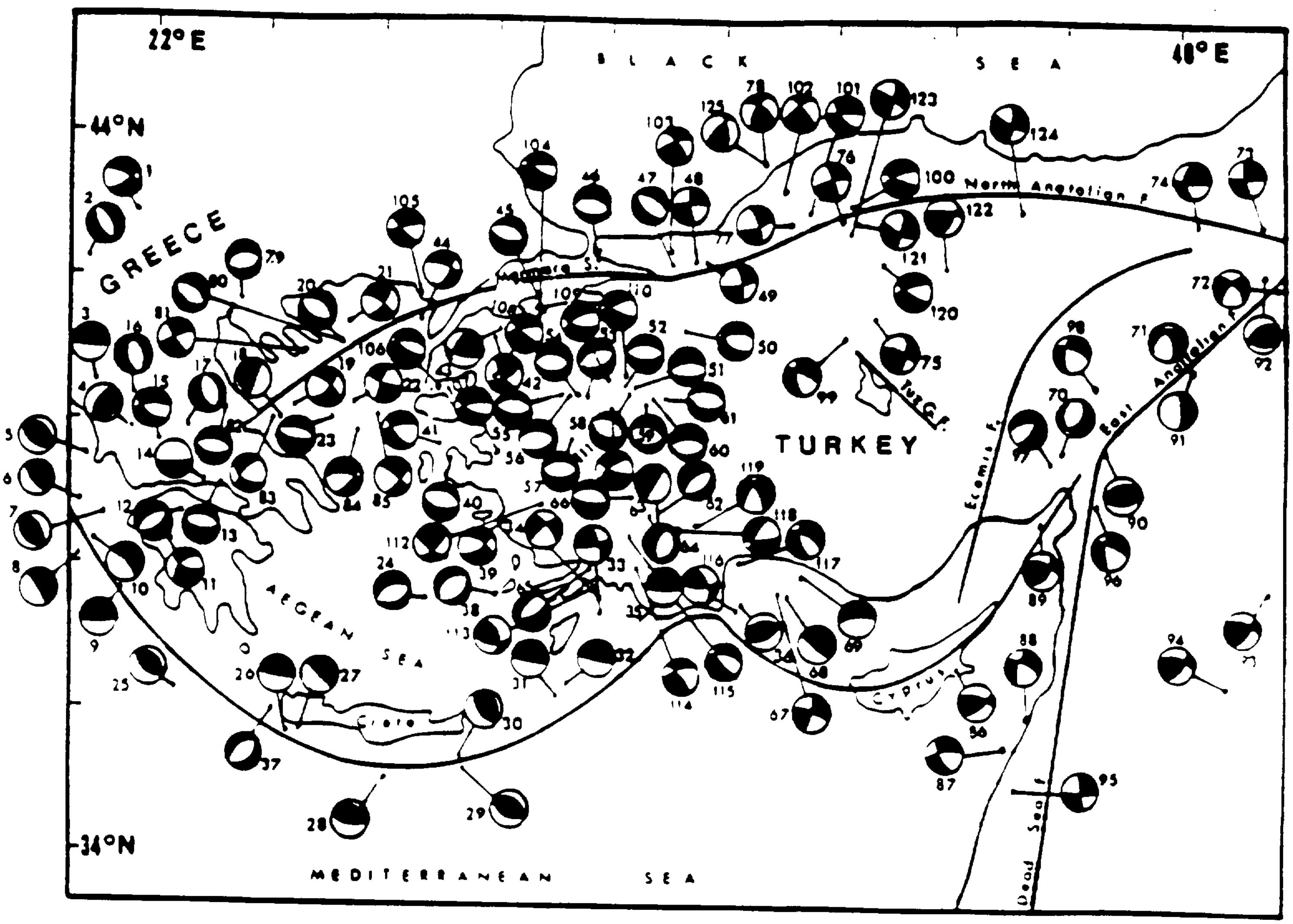

Figure 5 Fault plane solutions for earthquakes in the eastern Mediterranean (see Kasapoglu and Toksoz, 1983 for sources).

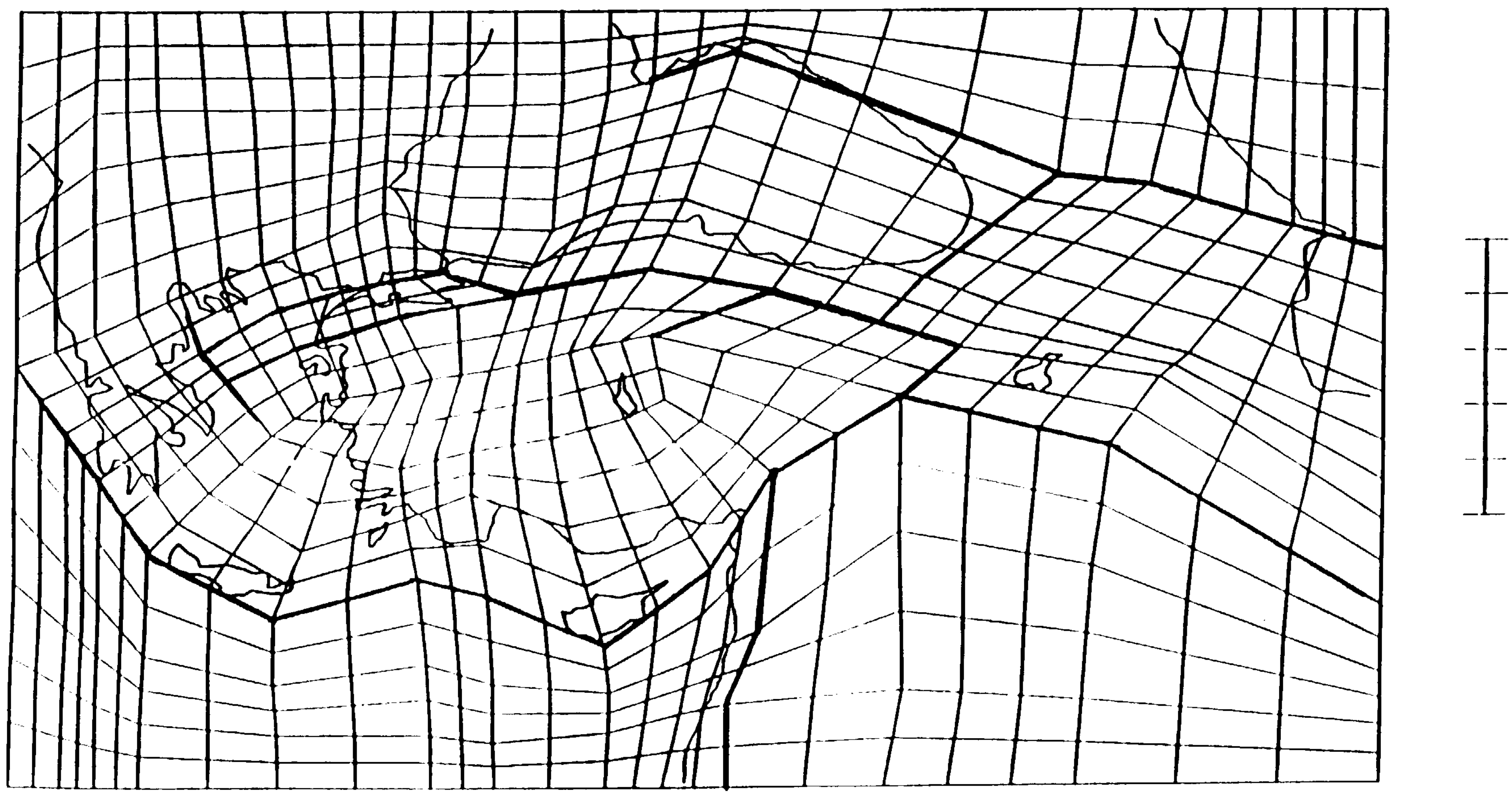

Figure 6. Grid used in finite element models of Eastern Mediterranean region.

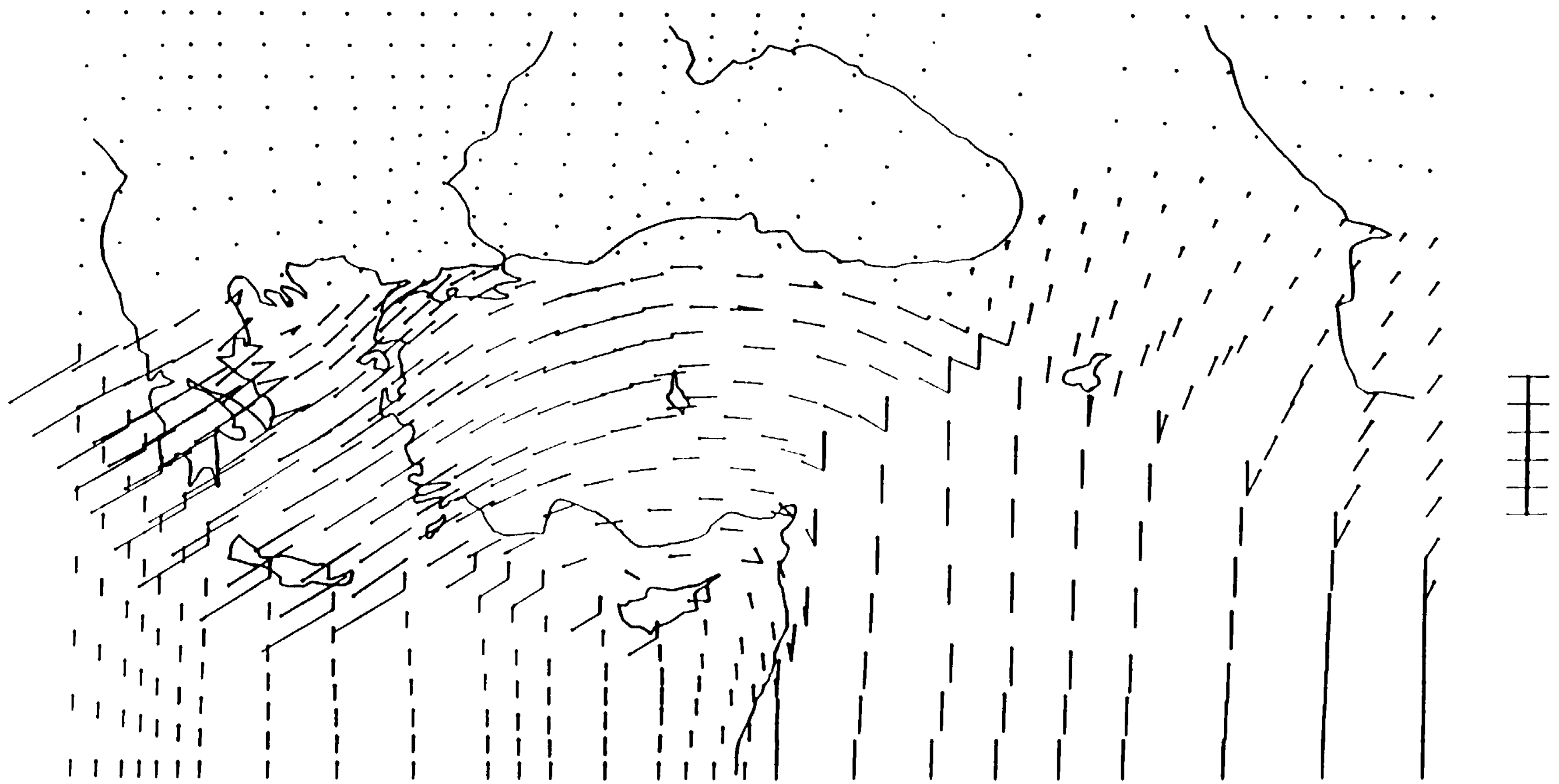

Figure 7. Modeled displacements for the Eastern Mediterranean region.

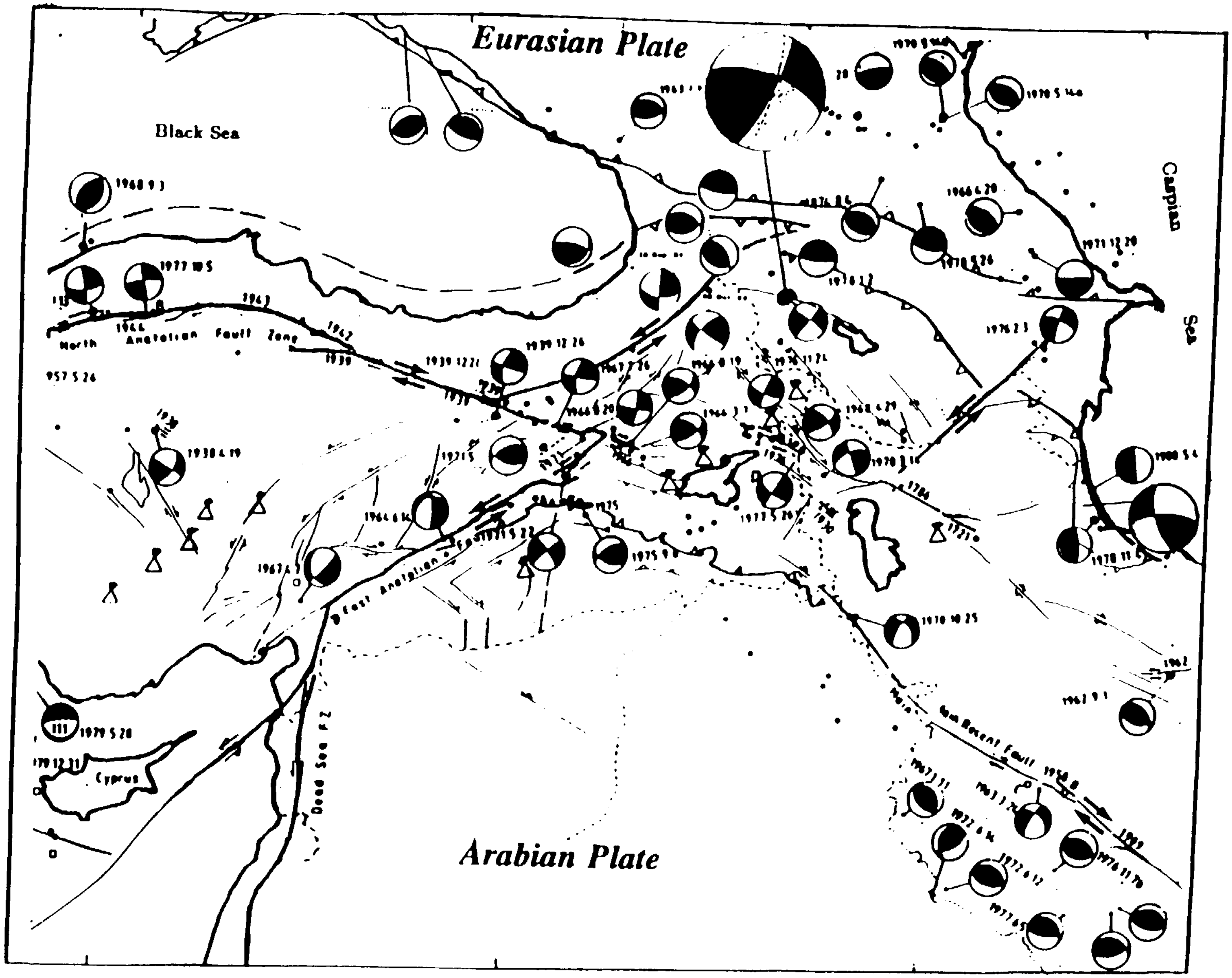

Figure 8 . Earthquake mechanisms in central and eastern Anatolia, western Iran, and Caucasia.

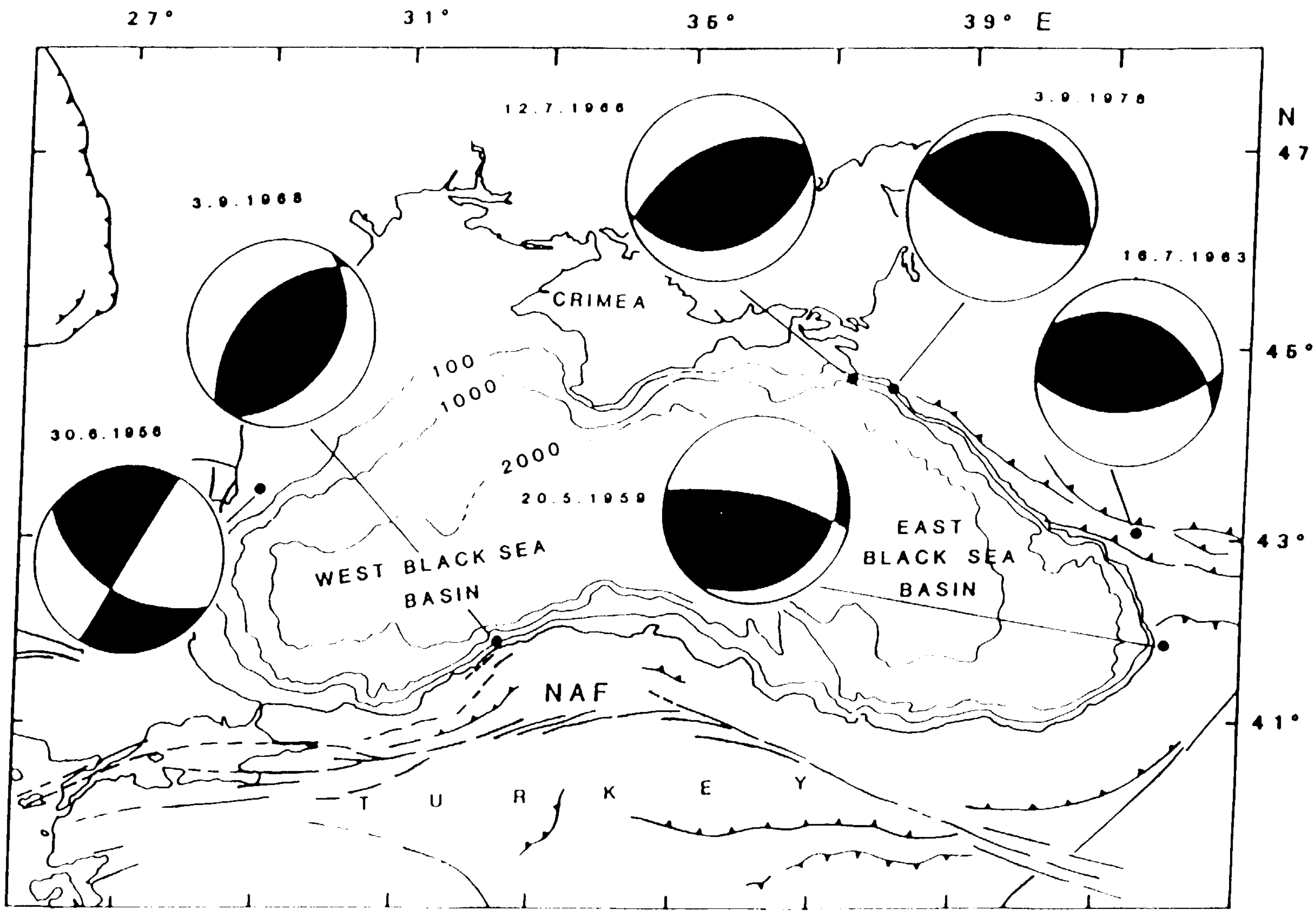

Figure 9 . Source Mechanisms of major earthquakes around the Black Sea. Note the thrust mechanism both on the northeast and southern margins. (After Alptekin et al, 1986)

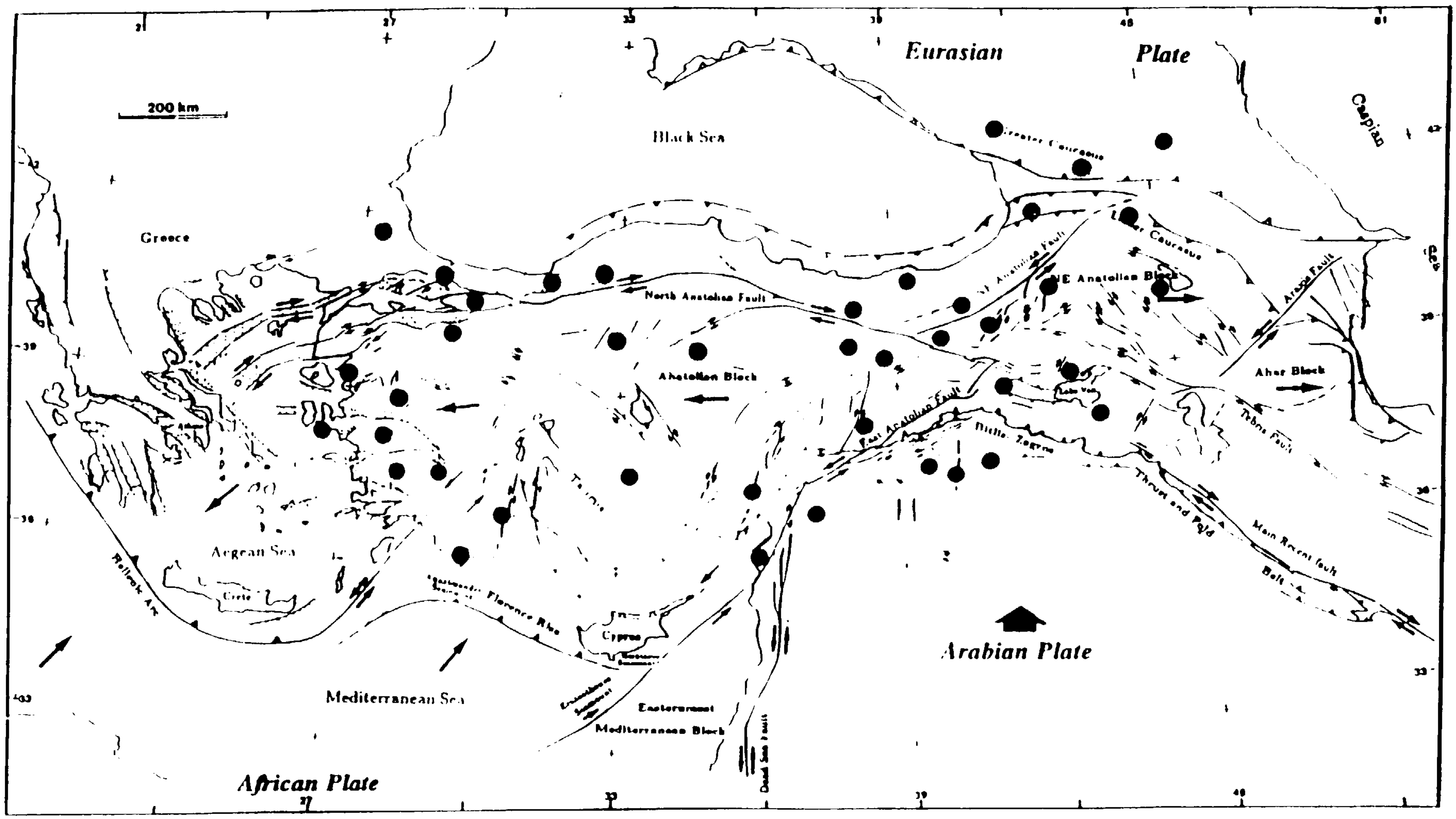

Figure 10. GPS sites established by MIT/TUJJB. Six sites in extreme NE were established by MIT/Indiana U. and IPE in 1991 (see text).

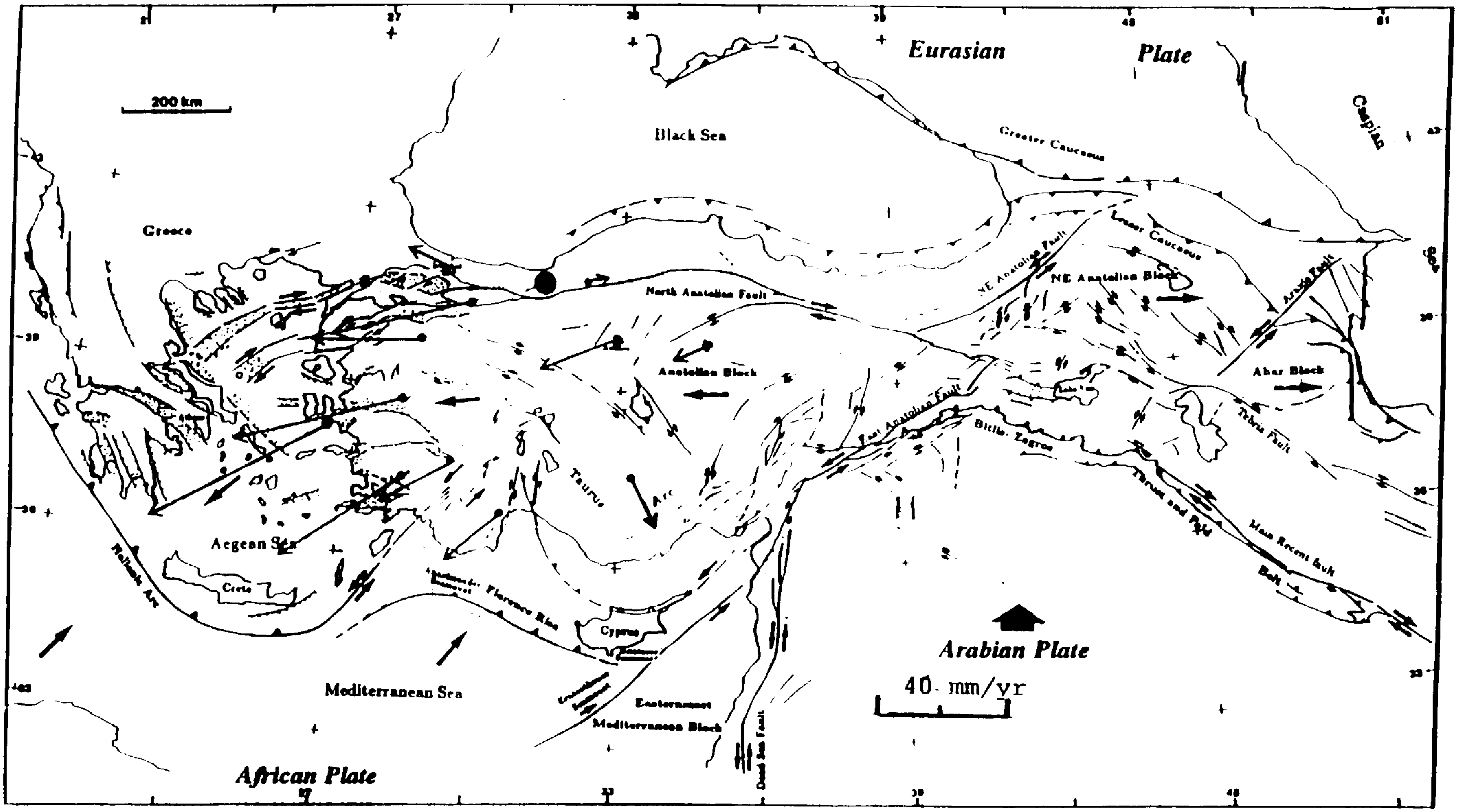

Figure 11. Displacements (1988-1990) in western Turkey from GPS.

APPENDIX I

(Submitted to AGU-CDP Monograph, 1992)

Preliminary Results of 1988 and 1990 GPS Measurements in Western Turkey and their Tectonic Implications

M. Burc Oral, Robert E. Reilinger and M. Nafi Toksöz

Earth Resources Laboratory,

Department of Earth, Atmospheric, and Planetary Sciences,

Massachusetts Institute of Technology,

Cambridge, MA 02139, USA.

Abstract

We present the first results of GPS measurements of regional crustal deformation in Turkey. The 1988 and 1990 GPS data from western Turkey were processed using the GAMIT and GLOBK packages. Derived "two-epoch-velocities" show a $\sim 25 \pm 9$ mm/yr right lateral motion across the North Anatolian Fault (NAF). Western Turkey moves southwest relative to the Eurasian plate at a rate of approximately 50 ± 20 mm/yr. Deformation models where plate boundaries are expressed as contacts show that forces created by the collision of the African and Arabian plates with Eurasia are insufficient to explain the high rates of deformation indicated by GPS observations in western Turkey and SLR observations along the Hellenic arc. Southward migration of the Hellenic arc due to either "trench suction" or mantle convection induced by the down-going slab may account for the extra force driving the fast extrusion of southwestern Turkey. The relatively high elevation of eastern/central Turkey may also contribute to the rapid extrusion of western Turkey.

Introduction

Deformation in the Eastern Mediterranean is controlled by the interaction of three plates—the African, Arabian and Eurasian plates. The bulk of the deformation in eastern Turkey is caused by the differential motion between the African and Arabian plates against the Eurasian plate, which manifests itself in the Bitlis and Caucasus convergent zones and crustal escape along strike-slip faults. This picture is compounded by extensional regimes in the

Aegean and western Turkey, subduction at the Hellenic and Cyprean arcs, and possible subduction in the Black Sea.

SLR station coverage in the Eastern Mediterranean provides information on broad-scale plate motions, but is not sufficiently dense to delineate the details of deformation associated with ongoing continental collision. A GPS geodetic network has been established in Turkey to determine the rates and directions of relative plate motions and the internal deformation of the Anatolian plate. The collected phase and group delay data from the 1988 and 1990 occupations in western Turkey were subjected to preliminary analyses using the GAMIT processing and the GLOBK adjustment packages; "two-epoch-velocities" were obtained. Our initial results provide the first quantitative estimates of present-day right-lateral strike slip motion across the central segment of the North Anatolian Fault and the southwest escape of western Turkey.

Incorporating plate boundaries as contacts, we develop a finite element modeling scheme that facilitates the interpretation of GPS and SLR measurements of crustal motions and provides a basis for investigating the dynamics of this complex region. These models demonstrate that N-S shortening across the collision zone is not sufficient to explain the observed deformations in western Turkey. Southward migration of the Hellenic trench and the extrusion of the Anatolian block are required to match Nuvel-1 plate velocities, SLR derived velocities at the Hellenic arc, and GPS site velocities.

Tectonic Background

Several authors have reported on the various geological and geophysical aspects of the Eastern Mediterranean where a number of coexisting tectonic regimes are confined (Figure 1): a continent-continent collision zone (Bitlis-Zagros, Caucasus), an extensional province (western Turkey, northern Aegean Sea, southern Greece), major transform faults (the North, Southeast and Northeast Anatolian Faults, Dead Sea Fault) and different stages of subduction (the Hellenic Arc, Black Sea).

Şengör and Yılmaz (1981), Robertson and Dixon (1984), Şengör (1987), and Gealey (1988), provide a review of the geological evolution of the Eastern Mediterranean within the Alpine-Himalayan orogenic belt and of its collisional development. The seismicity, deep structure and active tectonics of the region are summarized in a number of studies (e.g., McKenzie, (1970, 1972); Jongsma 1975; McKenzie, 1976; Morelli, 1978; Papazachos and Comminakis 1978; McKenzie,1978; Lort, 1978; Şengör, 1979; Canıtez and Toksöz, 1980; Lyberis, 1984; Makris and Stobbe, 1984; Jackson and McKenzie, 1984; Şengör *et al.*, 1985; Hempton, 1987; Barka and Kadinsky-Cade, 1988; Jackson and McKenzie, 1988; Philip *et al.*, 1989; Westaway, 1990).

Present-day tectonic deformation (neo-tectonics) of the region is closely related to the northerly motion of the Afro-Arabian plate and medial to late Eocene events in the Red Sea (Hempton, 1987). During this period Africa and Arabia formed a single plate and the continental margin of the Arabian platform collided with the Eurasian plate, closing the back arc basin of the Tethys. Thus, suturing began as subduction of Africa beneath Eurasia continued. As this process progressed into the early Miocene, the extension in the Red Sea and Gulf of Aden was accommodated by the separation of Arabia from Africa, resulting in the rapid convergence of the Arabian plate against Eurasia. Contemporaneously, the Dead Sea Fault initiated. By medial Miocene, the wide continental margin of Arabia was consumed, arresting its independent northerly motion. Subsequently, the first phase of extension in the Red Sea came to an end, as did the left-lateral motion along the Dead Sea Fault. Arabia and Africa, however, continued moving northward as a single plate causing excessive crustal thickening and shortening, and uplift in the convergent zone, until early Pliocene. The resulting convergent stresses were alleviated by the extrusion of continental wedges along transform faults (McKenzie, 1972) . Therefore, between late Miocene and early Pliocene, Anatolian strike slip faults (the North, Northeast, and Southeast Anatolian Faults) were initiated (Şengör, 1979; Barka and Hancock, 1984) and the Anatolian plate started to wedge out of the zone of maximum compression. Such escape tectonics along transforms triggered Arabia to move independent of Africa. Consequently, the second stage of the Red Sea's opening commenced, providing a faster convergence rate for the Arabian plate.

Global models for present-day plate motions using spreading rates, earthquake slip rate vectors, and transform fault azimuths show that the Arabian plate converges against Eurasia faster than the African plate (Minster and Jordan, 1978; Chase, 1978; Gordon and Jurdy, 1986; De Mets *et al.*, 1990). The differential motion between Arabia and Africa with respect to stable Eurasia, taken up along the Dead Sea Fault, amounts to 15–17 mm/yr (from De Mets *et al.*, 1990). The African plate, which has been continuously moving northward relative to Eurasia since 95 Ma, converges on Eurasia at 11 mm/yr (from De Mets *et al.*, 1990). The Nuvel-1 data for the relative motion of Eurasia and Africa are obtained from the Azore-Gibraltar ridge, and that for Arabia and Africa come from the Sheba ridge. Because there are no data for the relative motion between Eurasia and Arabia, their relative motion is indirectly calculated from plate circuits. The data for Eurasia-Africa relative motion are from outside the Mediterranean. Since the Nubia-Somalia motion is neglected, the spreading rates from the Red Sea do not constrain the Arabia-Africa motion. Further problems arise with the diffuse nature of regional continental deformation where the rigid plate assumption becomes less valid (McKenzie, 1977). The indirect methods of estimating plate motions in the Eastern Mediterranean and their probable uncertainties are important reasons for using SLR and GPS to obtain direct measurements of plate motions.

The Arabian plate convergence against Eurasia created two tectonic flakes—the Van block (Iran plate) and the Anatolian plate (Figure 1). Bounded by the Caucasus and the Bitlis-Zagros sutures, and by the North, Northeast and Southeast Anatolian transforms, the Van block escapes eastward. The Anatolian plate continues to accommodate shortening by westward drift along the right-lateral North and left-lateral Southeast Anatolian Faults. The estimated rate of slip across the North Anatolian Fault from earthquake and geologic studies is quite uncertain, with values reported between 5 and 30 mm/yr (e.g., Şengör, 1979;

Jackson and Mckenzie, 1984; Barka and Kadinsky-Cade, 1988). West of the Mudurnu Valley the North Anatolian Fault gains an extensional component (Barka and Kadinsky-Cade, 1988) and this feature becomes dominant in the North Aegean Trough (Lyberis, 1984). Although the central province of the Anatolian plate manifests relatively little internal deformation, the western province (western Turkey) is rich with extensional features. The Büyük and Küçük Menderes Breakaway Zones, their cross horsts and grabens (Şengör *et al.*, 1985) demonstrate N-S and E-W extension, respectively.

The bulk of the deformation in the region appears to have originated from the collisional process, i.e., the forces applied at the plate boundaries. However, the driving forces for the present-day escape, as speculated by Şengör *et al.* (1985) may also include forces caused by gravitational potential and/or basal traction.

Space Geodetic Measurements

SLR measurements

The WEGENER-MEDLAS (Working Group of European Geoscientists for the Establishment of Networks for Earthquake Research Mediterranean Laser Ranging) project (Reinhart *et al.*, 1985), which began in 1985, was the first step toward providing geodetic data that quantifies the deformations in this very active region. The first observational campaign started in 1986. Four sites in Turkey were visited during the third campaign: one site north of the North Anatolian Fault (Yığılca), two sites on the Anatolian plate (Yozgat and Me-

Yenigiçlik), and another on the Arabian plate (Diyarbakır) (see Figure 1). In 1988 and 1990 these sites were occupied with mobile LRS (Laser Ranging System) and laser range measurements to LAGEOS were performed. Analyses of these normal point data (Sellers *et al.*, 1991; Noomen *et al.*, 1991; Wakker *et al.*, 1991; Cenci *et al.*, 1991) show a 20 ±10 mm/yr right lateral motion across the North Anatolian Fault and a 50 ± 20 mm/yr southwest motion of Aegea relative to Eurasia.

GPS measurements

In 1988 M.I.T., with support from UNAVCO and in collaboration with Hacettepe University, initiated GPS measurements in Turkey to establish fourteen sites primarily in western and central Turkey (Figure 1). During this campaign, GPS measurements were also made at the four mobile SLR stations established in Turkey by WEGENER-MEDLAS.

During the summer/fall of 1990, regional GPS surveys were undertaken by M.I.T., IFAG, and ETH-Zurich in collaboration with Turkish Union of Geodesy and Geophysics (TUJJB). During this campaign the M.I.T. group reobserved ten GPS sites in western Turkey that had been established in 1988 (Figure 1). Simultaneous observations were carried out by IFAG at three SLR sites in central Turkey.

GPS campaigns were also undertaken in 1989 and 1991 by M.I.T. and Turkish collaborators which focused on deformation in the collision zone of eastern Turkey and neighboring areas in the Trans-Caucasus (Reilinger *et al.*, 1991). Figure 2 shows all GPS sites established by the M.I.T. group for the period 1988–1991. Data from the eastern Turkey campaigns are not included in this study.

Data

Figure 1 shows GPS sites common to the 1988 and 1990 campaigns. Baselines in the western Turkey network range from 95 km to 1200 km. with an average baseline length of 350 km. In both campaigns. observations were made at thirteen sites: Akdağ. Ankara. Antalya. Çesmeılıca. Çine. Kandilli. Ismetpaşa. Mekece. Melengiçlik. Pamukkale. Uludağ. Yığılca and Yozgat. No repeat observations at the Ayvalık. Demirköy. Diyarbakır. Kaş and Ödemiş sites were taken in 1990, although their occupation is planned for 1992. All receivers and antennas used for the 1988 survey were TI-4100s. The repeat experiment used a mixture of TI4100. MiniMac. and Trimble 4000s (SST and SLD), introducing asynchronous and irregular sampling of phase and group delay. During the experiments. selective availability was off and anti-spoofing was not introduced. In 1988 only six satellites were available (prns 3. 6. 9. 11. 12 and 13). The repeat experiment observed four additional new satellites (prns 2. 16. 18 and 20).

GPS Data Processing

The GAMIT software package (King and Bock. 1991; King *et al.*. 1985) was used to process the 1988 and 1990 GPS data. GAMIT is a suite of programs that fulfills a number of tasks, such as: (1) converts the field data into internal formats: (2) generates tabulated reference orbits and their partials for satellites from broadcast/adjusted ephemerides with a celestial model: (3) calculates the theoretical observations based on a geometrical model: (4) determines partial derivatives and differences from observed phase measurements: (5) detects outliers and gaps, and edits one-way data: and (6) estimates three-dimensional relative positions of observational sites and orbits, and atmospheric clock and ambiguity parameters from a weighted least squares analysis of phase delay measurements at the GPS frequencies. A simple flow chart of GAMIT software is given in Figure 3.

Solutions are carried out in the SV5 reference frame (Murray, 1991) derived from VLBI (GLB659) and SLR (CSR8902) with the AM1-2 hot spot model (RM2). Carrier beat phase observables and pseudoranges are used, and geometric terms are modeled (King *et al.*, 1985; Feigl, 1991). Sea level conditions are applied to determine the atmospheric delay at the zenith. The Saastamoinen (1972) model is applied for dry and wet zenith delay. The mapping function for delays is defined by Davis *et al.* (1985). Ionospheric delay is not included in the model: however it is calculated explicitly at the solution stage by estimation or application of the LC observable, or a combination of both as an ionospheric constraint.

Satellite clock parameters (offset, rate and acceleration) are modeled with a quadratic polynomial. No relativistic effects are included. Receiver clock parameters (offset, rate, acceleration and rate of acceleration) are estimated from pseudoranges epoch by epoch using a cubic polynomial with jumps.

Merit standards with an updated GM value and IERS tables are used for orbits and expressed in an inertial coordinate system. Perturbed satellite motion is defined with six osculating elements (cartesian position and velocity). The earth's gravity field is determined by the GEM-L2 model up to degree and order 8. The gravitational attraction of the sun and moon are considered. Non-gravitational parameters acting on the satellites are absorbed in the direct radiation pressure, x-axis and y-axis biases. A tabular ephemeris is integrated for each session at intervals of 22 minutes. For a single session the short-arc solution orbital trajectory is $\sim$ 12 hours long. For a long-arc single session "global" solution, 3–4 day long orbital trajectories are integrated and applied to a single day solution.

Removal of outliers and cycle-slip repairs are performed automatically with one-way, between-satellite difference, and using double difference data. Manual editing under X-windows is routinely practiced to eliminate cycle-slips overlooked during the automatic cleaning procedure.

A weighted least-square scheme is used to estimate the delays in the propagation medium, clock and ambiguity parameters (wide-lane [L2-L1] and narrow-lane [L1] biases), 3-D site positions, and satellite state vectors (six Keplerian elements, three non-gravitational parameters). Each single day solution consists of four steps (Feigl, 1991). First, all ambiguity parameters are set free and the ionosphere-free observable LC is used to estimate all the parameters (Bock *et al.*, 1986). Second, keeping all the parameters other than those whose ambiguities are fixed to the values obtained in the earlier step, wide-lane biases are estimated to fix the ambiguity parameters to integers. L1 and L2 phases, and wide-lane combinations (if and when pseudoranges are available) are used in this step. Third, narrow lane biases are estimated. The last step involves solving for all the parameters except wide-lane and narrow-lane biases which were successfully fixed to an integer. This is a "biases-fixed" solution. Biases-fixed and biases-free solutions are repeated for sufficiently loose constraints to obtain estimates and variance-covariance matrices as an input to the "global" solution.

A global solution requires estimates and variance-covariance matrices of long-arc single session solutions. The GLOBK software package (Herring *et al.*, 1990; Herring, 1991), a Kalman filter program, combines the variance-covariance matrices of these solutions to estimate the 3-D site positions and velocities, satellite state vectors, and earth orientation parameters (polar motion and UT1-UTC).

Application to Data

The Onsala, Richmond, Wettzell, Westford, Tromso, and Yellowknife CIGNET sites were used as fiducials in processing the 1988 campaign. The repeat campaign lacks Yellowknife and Tromso data due to data outages. Single day short-arc solutions have approximately 12 hour long orbits. Though the fiducial concept has been followed, instead of fixing fiducial site positions, we applied tight constraints on their positions (1–10 mm). Global solutions are performed with 3–4 day long arcs. Using the GLOBK package, precise determination of satellite state vectors, adjustment of site coordinates, and estimation of velocities are attempted.

The solutions presented are not "biases-fixed" and may still suffer from inhomogeneous fiducial site distribution and unconstrained orbital parameters. Repeatability in the east, north, and vertical is 10–30 mm + 1 parts in 10^8.

Preliminary Results of GPS Data Processing

To understand the interaction between the Eurasian, African and Arabian plates, site velocities expressed relative to the Eurasian plate provide a favorable frame of reference that can be conveniently described by the Onsola, Tromso and Wettzell sites. The baseline lengths between these and local sites are on the order of a few thousand kilometers. Thus, their relative errors, which translate to decimeters, do not allow the local sites' velocities to be resolved. Therefore, we adopt the frame defined by the Yığılca site which expresses "two-epoch-velocities" relative to the northern block of the NAF. This approach can be tested by examining the relative motions at Ismetpaşa, a site 25 km east of Yığılca, also located north of the NAF. Since there is no significant motion at Ismetpaşa at 95% confidence intervals, we conclude that rates obtained relative to Yığılca represent an adequate frame of reference. Furthermore, SLR solutions indicate no significant motion of Yığılca relative to stations in Europe (Ambrosius *et al.*, 1991), indicating that within the resolution of our measurements, Yığılca is a part of the Eurasian plate. Thus, the velocities derived in this study are in a fixed Eurasian plate reference frame.

Table 1 provides geocentric site coordinates (WGS84 datum), horizontal and vertical rates and their standard deviations and correlations. Figure 4 shows the "two-epoch-velocities" relative to Yığılca. The 95% confidence levels are high and vary between 10 and 20 mm/yr. Subsequently, rates are unresolvable at some sites due to the bias-free nature of the solution, residual orbital errors, and inadequate and non-homogeneous fiducial coverage.

The sense of motion indicated by the GPS rate vectors is generally consistent with those determined from geological observations. The magnitude and direction of GPS rate vectors are also consistent with some of those derived from SLR observations in the Aegean within their 95% confidence intervals, although some discrepancies remain between SLR solutions reported by various groups (e.g., Sellers *et al.*, 1991; Wakker *et al.*, 1991).

Right-lateral motion across the North Anatolian Fault is easily detectable, with the preliminary GPS estimate across this transform being 25 ± 9 mm/yr. The Anatolian block is rapidly escaping SW at a rate of 50 ± 20 mm/yr. The rates across the Marmara Sea demonstrate that the right-lateral motion continues westward. The significant motion at Kandilli, relative to Yığılca, may reflect the extensional character that NAF assumes west of the Mudurnu Valley. Higher velocities at Mekece and Uludağ also indicate that the motion across the southern branch of the western segment of the NAF is different from that on the central segment. Though relatively high confidence levels make it hard to resolve the N-S extension in western Turkey, there is at least a 10 mm/yr motion. A better estimate may be reached after the planned 1992 repeat measurement at the Ödemiş site on the Bozdağ Horst.

Modeling and Discussion

A finite-element modeling scheme, constrained by the SLR and GPS measurements of crustal motions as well as geological and seismological observations, was developed to investigate the kinematics and dynamics of the interaction between the Arabian, African, and Eurasian plates. The equation of equilibrium is solved for an aggregate of 2-D elastic plates (plane stress) in contact. A general potential energy equation in variational form is derived for frictional/tensional contacts (Oral *et al.*, 1991). It includes body forces, basal traction, ambient strain/stress, and variable plate thickness and is expandable to 3-D. This non-linear contact problem is iteratively solved for present-day plate velocities and forces arising at the contacts (Wang and Voigt, 1969). Similar contact algorithms (Bathe and Chaudhry, 1985; Chaudhry and Bathe, 1986; Bathe and Mijailovich, 1987) and joint element approaches (Goodman *et al.*, 1968; Goodman, 1975) are, in a broad sense, equivalent. Contacts are modeled with dual nodes, one node on each plate (Kasapoğlu and Toksöz, 1983). Compatibility is assured by Coulomb-Mohr failure criteria defined by three modes of contact allowing sudden velocity jumps across predefined boundaries—sticking (continuum), sliding (slip), and tension release (separation). The velocity field is discretized by 4-node quadrilateral serendipity elements. Gaussian quadrature integration is carried out at 3×3 Gaussian points.

Forces other than those at the contacts are ignored in the current models. Major plate boundaries are modeled as contacts: Dead Sea, North, Northeast, and Southeast Anatolian Faults, Aegean Trough, Aegean Block Faulting, Mediterranean Subduction, Arabian Collision Zone and Greater Caucasus Thrusting (Figure 5a). Due to the 2-D nature of the model, subduction can only be modeled explicitly such that the convergence across the Hellenic arc has to be specified. The contacts, assumed to be very weak, have almost no cohesion and have a low friction coefficient.

We have considered several deformational models on which Nuvel-1 velocities for Arabia and Africa relative to fixed Eurasia are imposed. The African and Arabian plates are assumed to be rigid with uniform velocities relative to the Eurasian plate of 11 mm/yr (at N 30, E 45) and 27 mm/yr (at N 30, E 35), respectively. These forcing conditions, applied on and within these plate boundaries define, by default, the deformations caused by the collision of Arabia against Eurasia, provided that the Anatolian block is treated as a separate plate and the Hellenic arc is explicitly modeled. The velocity field obtained from such a model underestimates the rate of deformation across the NAF and in western Turkey. Instead, we combine velocities obtained from GPS and SLR observations and model the Hellenic arc moving WSW at a rate of 60 mm/yr (30 mm/yr east of Kattavia SLR site, Rhodes), relative to Eurasia. This implies the application of some boundary forces on the overriding plate. Figures 5b and 5c show the velocity and strain fields, respectively for a model with Nuvel-1 plate motion and prescribed SW motion of the Hellenic arc. Sideways escape is remarkably dominant. Two contrasting strain regimes are noticed—extension in western Turkey and shortening in eastern Turkey. With an average strain rate of 8×10^{-6} yr^{-1}, the Van block escapes NE at $\sim$ 15 mm/yr. The motion across the NAF and SEAF is predicted to be $\sim$ 20 mm/yr. The contact along the NAF does not yield a pure slip mode. There is a component of tension release. The deformation across the NEAF is less than 10 mm/yr. Our models also predict an opening at the Karliova and Maras triple junctions, and in the Marmara Sea. The extensional regimes in the Aegean Sea and southern Greece are consistent with geological observations.

The velocity field is slightly lower than that of GPS, suggesting the necessity of modeling a region inclusive of the Aegean Sea, as well as the Hellenic arc, to produce GPS velocities in western Turkey. This implies that basal slip should be introduced to the models. Another option is to increase velocities at the Hellenic arc. This is done, however, at the expense of exceeding SLR determined velocities.

Comparison of Figures 4 and 5b indicates that the velocity at Melengiçlik deviates significantly from that predicted by our model. This may be due to the motion of the block bounded by the SEAF and the Teke wedge (the wedge is created as the Mediterranean subduction jumps from the Hellenic arc to the Cyprean arc). The boundaries of this block and wegde are not included in our models. Instead, a continuous boundary is assumed (Figure 5b). Although this is a deficiency in the current model, it shows how the contact approach, by allowing velocity jumps across boundaries, can correctly define the plate motions. A similar argument is valid for the breakaway zones and their cross horsts and grabens, whose features must be modeled as contacts in order to delineate the relative motion across each small block.

Conclusions

The GPS measurements in Turkey, combined with more widely spaced SLR coverage, provide valuable information for quantifying the diffuse deformation in the Eastern Mediterranean. Site velocities obtained by GPS agree with those of SLR within their 95% confidence levels. The accuracy of the velocities obtained from the 1988 and 1990 campaigns will be improved as the 1989 and planned 1992 campaign data are included in the analysis.

Site velocities obtained from two epoch measurements show a rapid escape of western Turkey along the Anatolian transform faults (50 ± 20 mm/yr). The relative motion found across the central segment of the NAF (25 ± 9 mm/yr) provides the first quantitative estimate of present-day strain accumulation with implications for seismic risk assessment in this heavily populated region. Likewise, the geodetic data show that the western segment of the NAF, splintered in several branches, is much more active than was expected. The rates obtained at Mekece may reflect the motions of the Gemlik block, which is bounded by these branches. The extensive deformation in and around Bozdağ Horst, quantified by GPS measurements, demonstrates the active extensional tectonics of this region.

Numerical models show that the deformation in western Turkey cannot be accounted for by collisional processes alone. A corner flow model driving the Aegea, combined with gravity driven processes (Wdowinski *et al.*, 1989), may explain the high rates of relative motion observed in western Turkey. It is shown that modeling plate boundaries as contacts across which sudden velocity jumps are allowed is an adequate technique to account for slip and tensional modes. The limitations posed by explicit modeling of dip slip can be removed by expanding to the full 3-D.

Acknowledgments

We are grateful to the members of Hacettepe University, the Turkish Irrigation Foundation(DSI) and the Turkish General Command of Mapping (HGK) for their sleepless nights spent in the field collecting GPS data. Majors İbrahim Kınık and Ömür Demirkol (HGK) assisted in the realization of the campaigns. Most of the geological field work was provided by Aykut Barka and complemented by Levent Gülen. We also thank Peter Wilson (IFAG, Germany) for providing GPS data at SLR sites. We thank Ernie Marion for making the CIGNET data available to us and Judah Levine for spending time with TI data translation. We have benefited from long discussions with Kurt Feigl, Mark Murray, and Da-nan Dong. Bob King and Tom Herring shared their knowledge, experience, and time during data processing. We will miss our talks and correspondence with the late Paul Sellers, and especially his "let the data determine everything" anecdote. Jane Maloof and Al Taylor at the M.I.T. Earth Resources Laboratory computing facilities helped us to "fix" our endless problems. We also thank Leah Crandall for editing the "never-ending" drafts. This research was supported in part by NASA Grants NAG5-753 and NAGW-1961, and NSF Grant EAR-8709461.

Figure Captions

Figure 1 : Tectonics of the Eastern Mediterranean region (after Şengör *et al.*, 1985, modifications by A. A. Barka). Sites occupied during the 1988 and 1990 campaigns are indicated by solid circles. Open circles show sites occupied in 1988 only. 1: Ankara, 2: Yozgat, 3: Melengiçlik, 4: Yığılca, 5: Ismetpaşa, 6: Mekece, 7: Kandilli, 8: Demirköy, 9: Uludağ, 10: Akdağ, 11: Ayvalık, 12: Ödemiş, 13: Çine, 14: Pamukkale, 15 : Kaş, 16: Antalya, 17: Diyarbakır, 18: Çesmelica.

Figure 2 : MIT GPS network in Turkey and Trans-Caucasus. Sites occupied between 1988 and 1991.

Figure 3 : Flow chart of GAMIT software.

Figure 4 : The "two-epoch-velocities" relative to Yığılca. Site velocities are obtained by combining variance-covariance matrices of long-arc single-day GAMIT solutions in GLOBK. Yığılca is denoted by a large dot.

Figure 5a : The finite-element discretization and plate boundaries as contacts. Solid lines show contacts: Dead Sea, North, Northeast, and Southeast Anatolian Faults, Aegean Trough, Aegean Block Faulting, Mediterranean Subduction, Arabian Collision Zone and Greater Caucasus Thrusting. Scale unit is meters.

Figure 5b : The velocity field. Boundary conditions: Eurasian plate is held fixed: Arabia and Africa move 27 mm/yr and 11 mm/yr relative to Eurasia. respectively; Hellenic arc moving WSW at a rate of 60 mm/yr (30 mm/yr east of Kattavia. Rhodes), relative to Eurasia. Arrows are at the end of the velocity vectors. At the contacts. there are two velocity vectors for each plate. Scale unit is meters.

Figure 5c : The strain field calculated at the Gaussian points of each [finite] element. Inward directed arrows indicate shortening. Scale unit is yr^{-1}.

Table 1 Horizontal and Vertical Rates ("two-epoch-velocities") relative to Yığılca. Site coordinates are geocentric.

SITE	Longitude (deg)	Latitude (deg)	Rates East (mm/yr)	North (mm/yr)	σ_{ee}	σ_{nn}	ρ_{en}	Rate Vertical (mm/yr)	σ_{v}
AKDAĞ	27.873	39.006	-55.0	-13.2	7.1	4.0	0.707	-122.2	10.2
ANKARA	32.726	39.871	-22.6	-10.6	3.2	1.6	0.581	-132.8	5.4
ANTALYA	30.583	36.822	-18.0	-14.7	7.1	3.7	0.585	-137.0	10.5
ÇEŞMEILICA	26.385	38.311	-58.1	-29.9	7.8	5.0	0.632	-142.9	9.5
ÇINE	28.081	37.609	-41.1	-27.0	6.9	4.3	0.651	-139.7	10.5
ISMETPAŞA	32.570	40.881	5.6	0.7	3.1	1.7	0.631	-128.8	7.2
MEKECE	30.026	40.465	-48.7	-10.0	5.6	2.9	0.756	-125.6	10.6
MELENGIÇLIK	33.191	37.378	8.1	-13.7	6.8	2.8	0.429	-21.3	10.9
KANDILLI	29.064	41.064	-13.7	5.2	4.4	2.6	0.705	-99.7	8.3
PAMUKKALE	29.136	37.941	-23.5	-12.5	7.0	3.8	0.675	-144.5	10.5
ULUDAĞ	29.141	40.122	-35.5	0.2	5.8	2.9	0.754	-150.3	8.8
YOZGAT	34.813	39.801	-10.2	-4.8	6.9	3.3	0.583	-108.4	10.0

REFERENCES

Ambrosius. B.A.C.. Noomen. R.. and K.F. Wakker. European station coordinates and motions from Lageos laser range observations. presented at the Crustal Dynamics Principal Investigators Meeting. Greenbelt. MD. Oct. 22–24. 1991.

Barka. A.A.. and P.L. Hancock. Neotectonic deformation patterns in the convex-northwards arc of the North Anatolian Fault. in *The Geological Evolution of Eastern Mediterranean. Spec. Publ.*. edited by J.G. Dixon and A.H.F. Robertson. 763–773. Geological Society of London. 1984.

Barka. A. and K. Kadinsky-Cade. Strike-slip fault geometry in Turkey and its influence on earthquake activity, *Tectonics*. *7*. 663–684. 1988.

Bathe. K-J. and A. Chaudhry. A solution method for axisymmetric contact problems. *Int. J. Num. Meth. Eng.*, *21*. 65–88. 1985.

Bathe. K-J. and S. Mijailovich. Finite-element analysis of frictional contact problems. *J. De Mechanique Theorique et Applique*. 375–389, 1987.

Bock. Y.. S.A. Gourevitch. C.C. Counselmann III, R.W. King and R.I. Abbot. Interferometric analyses of GPS phase observations. *Manuscr. Geod.*. *11*. 282–288. 1986.

Cenci, A.. M. Fermi. C. Sciarretta. R. Cardarelli, R. Devoti. R. Lanette. C. Luceri and G. Moliterni. Tectonic motion from Lageos data: The TPZ-90.2 solution. presented at the Crustal Dynamics Principal Investigators Meeting, Greenbelt. MD. Oct. 22–24. 1991.

Chaudhry. A. and K-J. Bathe. A solution method for static and dynamic analysis of three-dimensional contact problems with friction. *Comp. Struct.*, *24*, 885–873, 1986.

Canitez, N., and M.N. Toksöz, Crustal structure in Turkey, *EOS, Trans. Am. Geophys. Union*, *61*, 290, 1980.

Chase, C. G., Plate kinematics, The Americas, East Africa, and the rest of the world, *Earth Plaent. Sci. Lett.*, *37*, 355–368, 1978.

Davis, J.L., T.A. Herring, I.I. Shapiro, A.E.E. Rogers, and G. Elgred, Geodesy by radio interferometry: Effects of atmospheric modeling errors on estimates of baseline length, *Radio Science*, *20*, 1593–1607, 1985.

DeMets, C., Gordon, R. G., D. F. Argus, and S. Stein, Current plate motions, *Geophys. J. Int.*, *101*, 425–478, 1990.

Feigl, K.L., Geodetic measurement of tectonic deformation in central California, Ph.D. thesis, Massachusetts Institute of Technology, 222 pp., 1991.

Gealey, W.K., Plate tectonic evolution of the Mediterranean-Middle East region, *Tectonophys.*, *155*, 285–306, 1988.

Goodman, R.E., R.L. Taylor, and T.R. Brekke, A model for the mechanics of jointed rock, *J. Soil Mechanics and Foundations Division, Proceedings of the American Society of Civil Engineers*, *94*, 637–659, 1968.

Goodman, R.E., *Methods of Geological Engineering in Discontinuous Rock*, West Publishing Company, St. Paul, MN., 1975.

Gordon R. G. and D. M. Jurdy, Cenozoic Global Plate Motions, *J. Geophys. Res.*, *91*, 12389–12406. 1986.

Herring, T.A.. GLOBK: Global Kalman filter VLBI and GPS analysis program. unpublished documentation. Massachusetts Institute of Technology, 1991.

Herring, T. A., J. L. Davis. and I. I. Shapiro. Geodesy by radio interferometry: The Application of Kalman filtering to the analyses of very long baseline interferometry data. *J. Geophys. Res.*, *95*, 12561–12581. 1990.

Hempton. M.R.. Constraints on the Arabian plate motion and extensional history of the Red Sea, *Tectonics*, *6*, 687–705. 1987.

Jackson, J., and D.P. McKenzie. Active tectonics of the Alpine-Himalayan belt between western Turkey and Pakistan. *Geophys. J.R. astr. Soc.*, *77*, 185–246, 1984.

Jackson, J. and D. McKenzie. The relationship between plate motions and seismic moment tensors, and the rates of active deformation in the Mediterranean and Middle East. *Geophys. J. R. astr. Soc.*, *93*, 45–73, 1988.

Jongsma. D., A marine geophysical study of the Hellenic arc. Ph.D. thesis. University of Cambridge, 1975.

Kasapoğlu, K.E., and M.N., Toksöz. Tectonic consequences of the collision of the Arabian and Eurasian plates: finite element models. *Tectonophysics*, *100*, 71–95, 1983.

King, R.W., Y. Bock. Documentation for the M.I.T. GPS analysis Software: GAMIT. Release 8.2, Massachusetts Institute of Technology, 1991.

King, R.W.. J. Collins. E.M. Masters. C. Rizos. and A. Stolz. Surveying with GPS, Monograph No. 9. School of Surveying, The University of New South Wales. Kensington. N.S.W.. Australia. 132 pp.. 1985.

Lort. J.. Geophysics of the Mediterranean Sea Basins. in *The Ocean Basins and Margins.* edited by A.E.M. Nairn. W.H. Kanes. and F.G. Stehli. Plenum Press. New York. 151–213. 1978.

Lyberis. N.. Tectonic evolution of the north Aegean Trough. in *The Geological Evolution of Eastern Mediterranean. Spec. Publ..* edited by J.G. Dixon and A.H.F. Robertson. 711–725. Geological Society of London. 1984.

Makris, J., and C. Stobbe. Physical properties and state of the crust and upper mantle of the Eastern Mediterranean sea deduced from geophysical data. *Marine Geology, 55.* 347–363. 1984.

McKenzie. D.P.. Plate tectonics of the Mediterranean region. *Nature. 226.* 239–243. 1970.

McKenzie. D.P.. Active tectonics of the Mediterranean region. *Geophys. J.R. astr. Soc.. 30.* 109–185. 1972.

McKenzie. D.P.. The East Anatolian Fault: a major structure in Eastern Turkey. *Earth Planet. Sci. Lett.. 29.* 189–193. 1976.

McKenzie. D.P.. Can plate tectonics describe continental deformation. in International symposium on the structural history of the Mediterranean Basins. Split(Yugoslavia). 25–29 October 1976. edited by B. Biju-Duval. and L. Montadert. Editions Technip. Paris. 189–196. 1977.

McKenzie, D.P., Active tectonics of the Alpine-Himalayan belt: the Aegean Sea and surrounding regions, *Geophys. J.R. astr. Soc.*, *55*, 217–254, 1978.

Minster, J. B., and T. H. Jordan, Present-day plate motions, *J. Geophys. Res.*, *83*, 5331-5354, 1978.

Morelli, C., Eastern Mediterranean: Geophysical results and implications, *Tectonophys.*, *46*, 333–346, 1978.

Murray, M.H., Global Positioning System measurement of crustal deformation in Central California, Ph.D. thesis, Massachusetts Institute of Technology, 310 pp., 1991.

Noomen, R., B.A.C. Ambrosius, K.F. Wakker, Determination of station coordinates and motions from Lageos laser range observations, presented at the Crustal Dynamics Principal Investigators Meeting, Greenbelt, MD, Oct. 22–24, 1991.

Oral, M.B., M.N. Toksöz, and R.E. Reilinger, GPS measurements and finite element modeling of present-day tectonic deformations in the Eastern Mediterranean (abstract), AGU Chapman Conference, Time Dependent Positioning: Modeling Crustal Deformation, Sept. 23–25, 1991, Annapolis, MD.

Papazachos, B.C. and P.E. Comminakis, Deep structure and tectonics of the Eastern Mediterranean, *Tectonophys.*, *46*, 285–296, 1978.

Philip H., A. Cisternas, A. Gviskiani, and A. Gorshkov, The Caucasus: an actual example of the initial stages of continental collision, *Tectonophys.*, *161*, 1–21, 1989.

Reilinger, R.E., M.W. Hamburger, M.T. Prilepin, T.V. Guseva, Epoch geodynamic GPS measurements across the Caucasus Collision Zone. USSR (abstract). *EOS Trans. AGU.* 72, 112. 1991.

Reinhart. E., P. Wilson. L. Aardom. and E. Vermaat. The WEGENER Mediterranean Laser Tracking Project WEGENER-MEDLAS. CSTG Bulletin No. 8. Munich. F. R. G., 1985.

Robertson A.H.F., and J.G., Dixon Introduction: aspects of the geological evolution of the Eastern Mediterranean. *Geol. Soc. London. Spec. Publ.*, 1–74. 1984

Saastamoinen. J., Atmospheric correction for the troposphere and stratosphere in radio ranging satellites. in *The Use of Artificial Satellites for Geodesy Geophys. Monogr. Ser., 15,* edited by S.W. Henriksen. A. Mancini and B.H. Chowitz, 247–251, AGU. Washington D.C., 1972.

Sellers, P.C., P.N., Rands and P. Cross, Crustal deformation in Europe and the Mediterranean determined by analysis of Satellite Ranging Data. presented at the Crustal Dynamics Principal Investigators Meeting, Greenbelt. MD. Oct. 22-24. 1991.

Şengör. A.M.C., and Y. Yılmaz. Tethyan evolution of Turkey: a plate tectonic approach, *Tectonophys.*, *75*, 181–241, 1981.

Şengör, A.M.C., Tectonics of the Tethysides: Orogenic collage development in a collisional setting, *Ann. Rev. Earth Planet. Sci.*, *15*, 213–244, 1987.

Şengör, A.M.C., The North Anatolian transform Fault: its age, offset and tectonic significance. *J. Geol. Soc. Lond.*, *136*, 269–282. 1979.

Şengör, A.M.C., Görür, N., and F. Şaroğlu, Strike-slip faulting and related basin formation in zones of tectonic escape: Turkey as a case study, in *Strike-slip Faulting and Basin Formation*, edited by K.T. Biddle and N. Christie-Blick, *Society of Econ. Paleont. Min. Sec. Pub.*, *37*, 1985.

Wakker, K.F., B.A.C. Ambrosius, R. Noomen, B.H.W. van Gelder, and E. Vermaat, Combined analysis of Lageos II and Lageos I SLR data, presented at the first LAGEOS II Principal Investigators Meeting, Goddard Space Flight Center, Greenbelt, MD, Oct. 21, 1991.

Wang, Y.J., and B. Voigt, A discrete element stress analysis model for discontinuous materials, Proceedings of the International Symposium of Large Permanent Underground Openings, pp. 112–115, 1969.

Wdowinski, S., R.J. O'Connell, and P. England, A continuum model of continental deformation above subduction zones: Application to the Andes and the Aegean, *J. Geophys. R.*, *94*, 103311–10346, 1989.

Westaway, R., Block rotations in western Turkey, 1. Observational evidence, *J. Geophys. R.*, *95*, 19857–19884, 1990.

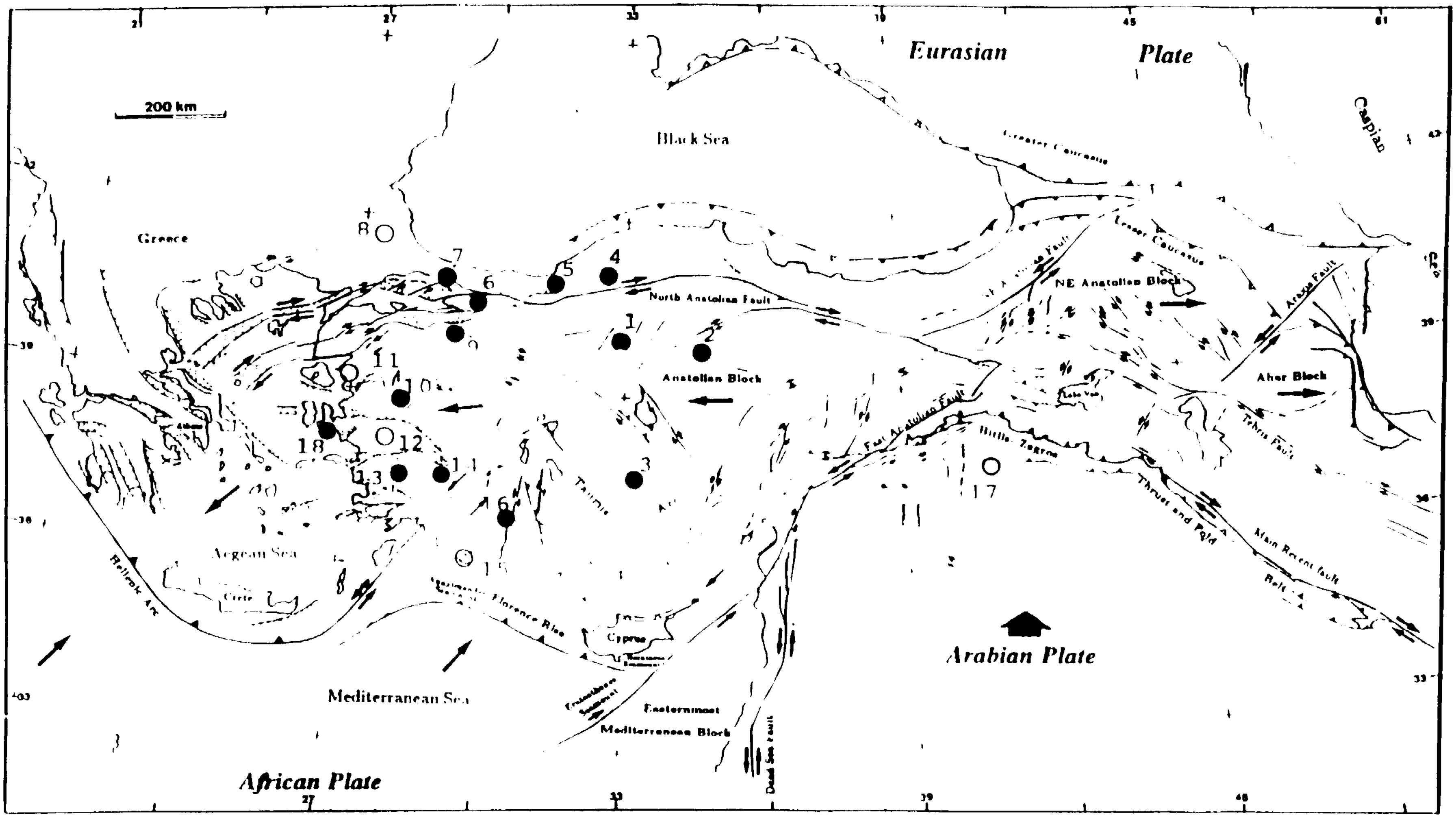
Eurasian
Plate
200 km
Black Sea
Greece
Caspian
Greater Caucasus
Lesser Caucasus
NE Anatolian Block
North Anatolian Fault
Anatolian Block
East Anatolian Fault
Aher Block
Tebriz Fault
Araxe Fault
Thrust and Fold
Main Recent fault
Aegean Sea
Crete
Hellenic Arc
Florence Rise
Cyprus
Mediterranean Sea
Easternmost
Mediterranean Block
Dead Sea fault
African Plate
Arabian Plate
1
2
3
4
5
6
7
8
11
12
13
16
17
18

FIG. 1

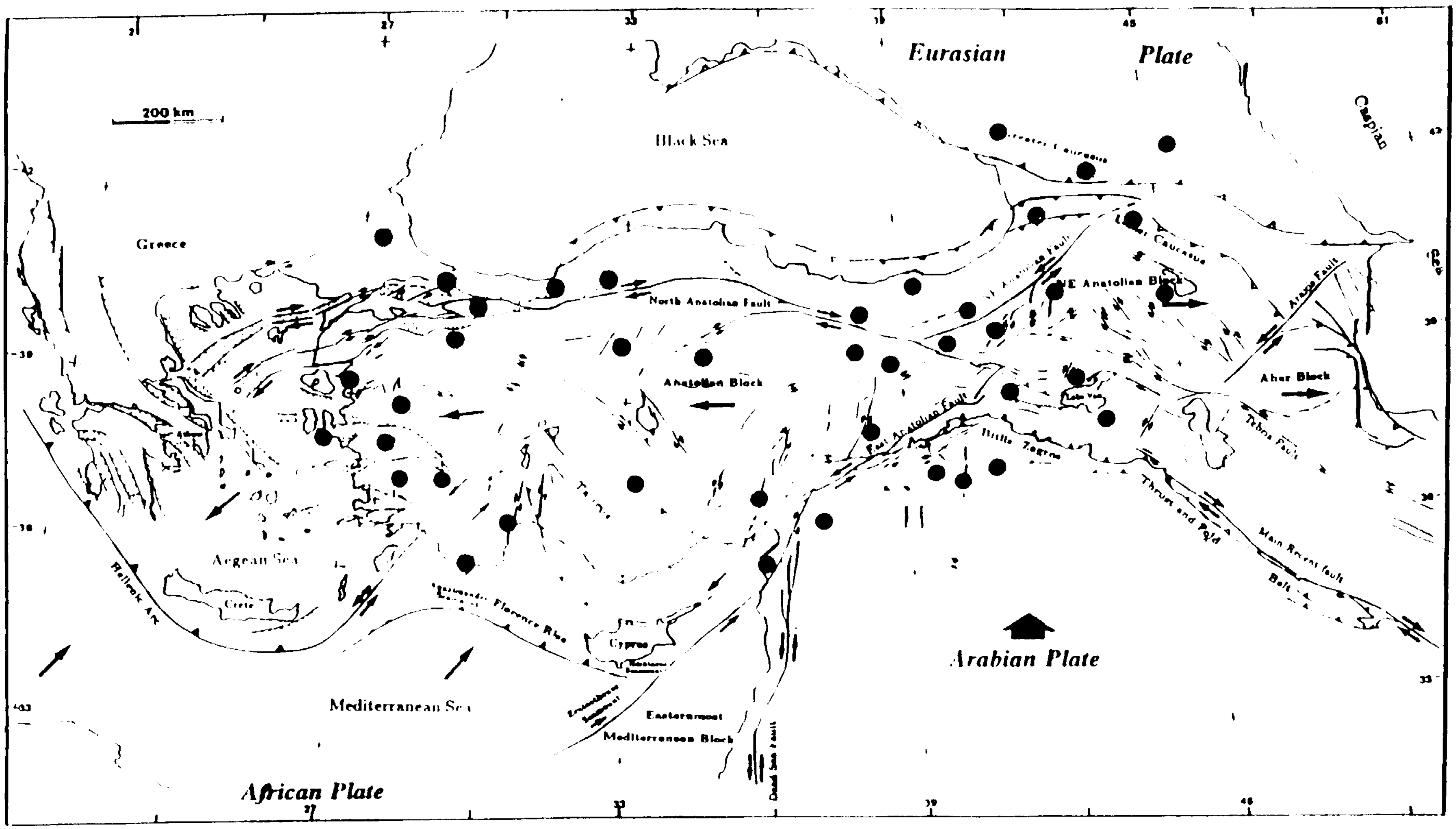

Eurasian Plate
200 km
Black Sea
Greece
Caspian
North Anatolian Fault
NE Anatolian Block
Anatolian Block
Ahar Block
East Anatolian Fault
Tebriz Fault
Aegean Sea
Crete
Hellenic Arc
Florence Rise
Cyprus
Thrust and Fold Belt
Main Recent fault
Arabian Plate
Mediterranean Sea
Eastern Mediterranean Block
Dead Sea Fault
African Plate

FIG 2

GAMIT

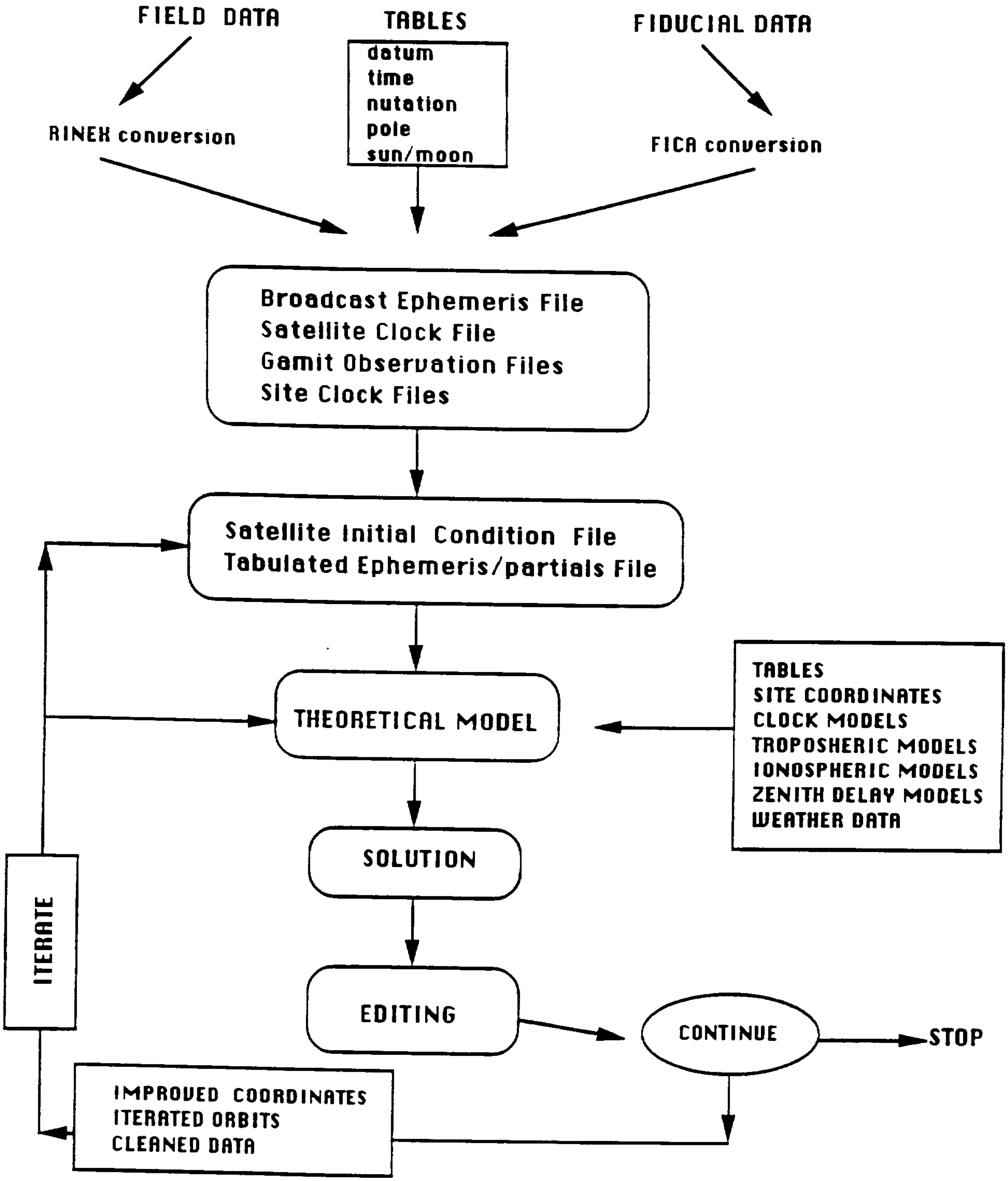

FIELD DATA
TABLES
FIDUCIAL DATA
datum
time
nutation
pole
sun/moon
RINEX conversion
FICA conversion
Broadcast Ephemeris File
Satellite Clock File
Gamit Observation Files
Site Clock Files
Satellite Initial Condition File
Tabulated Ephemeris/partials File
THEORETICAL MODEL
TABLES
SITE COORDINATES
CLOCK MODELS
TROPOSHERIC MODELS
IONOSPHERIC MODELS
ZENITH DELAY MODELS
WEATHER DATA
SOLUTION
EDITING
CONTINUE
STOP
ITERATE
IMPROVED COORDINATES
ITERATED ORBITS
CLEANED DATA

FIG 3

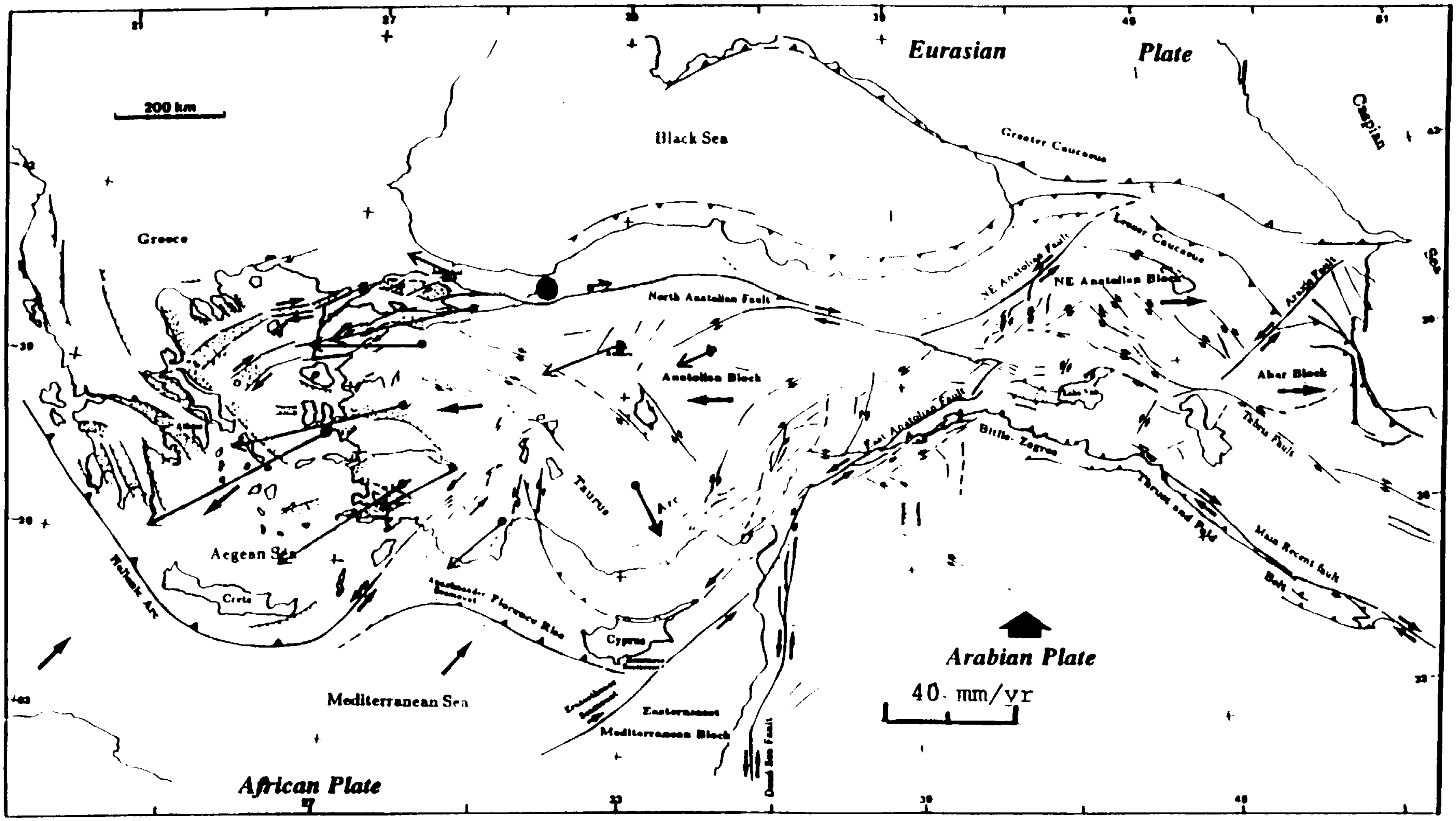
200 km
Eurasian
Plate
Black Sea
Greater Caucasus
Lesser Caucasus
Caspian
Greece
North Anatolian Fault
NE Anatolian Fault
NE Anatolian Block
Anatolian Block
Ahar Block
Tabriz Fault
East Anatolian Fault
Bitlis Zagros
Thrust and Fold
Belt
Main Recent fault
Taurus
Arc
Aegean Sea
Crete
Hellenic Arc
Florence Rise
Cyprus
Eastern Mediterranean Block
Dead Sea Fault
Mediterranean Sea
African Plate
Arabian Plate
40. mm/yr

FIG 4

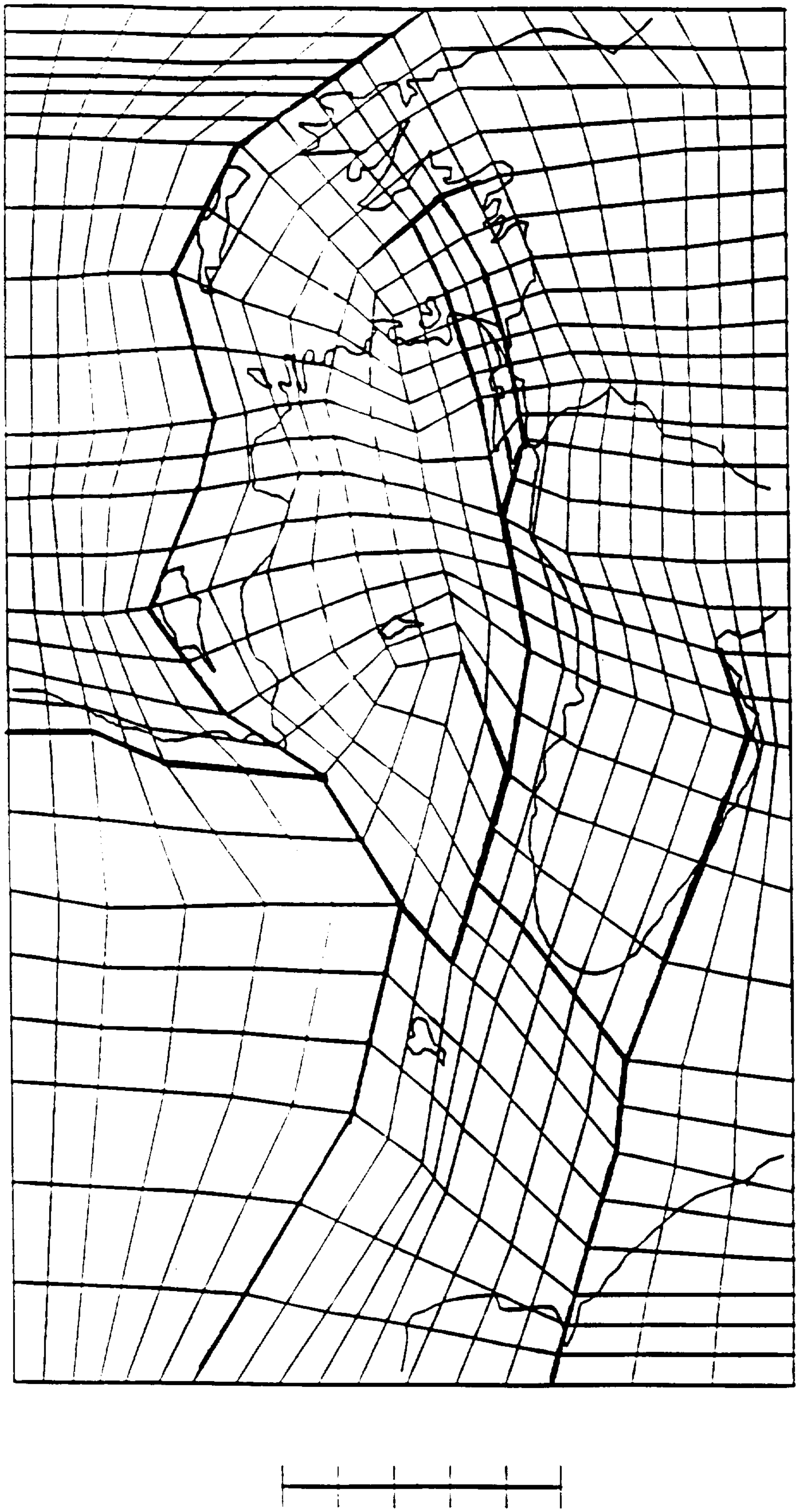

Fig.5a

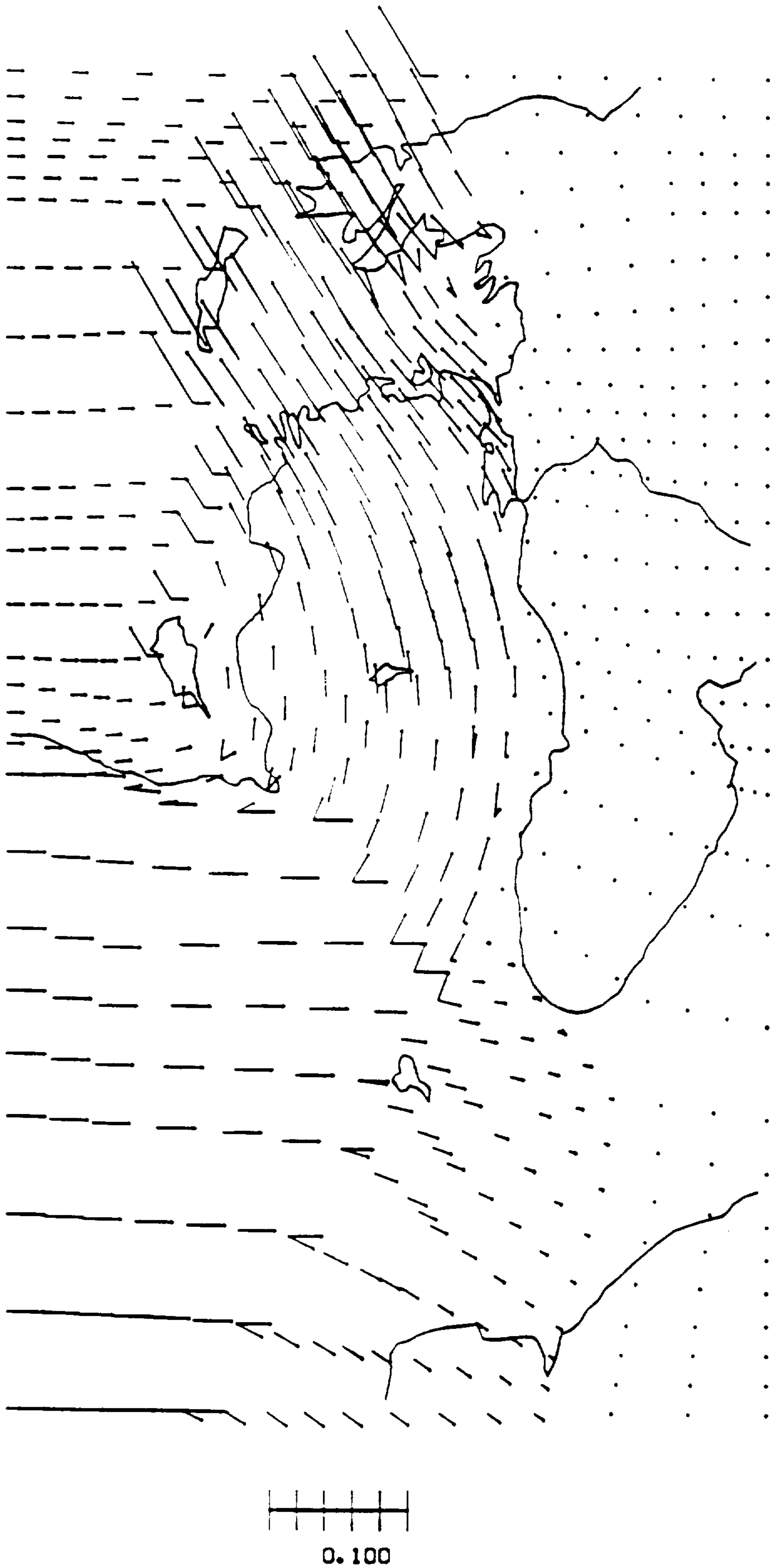

FIG 5b

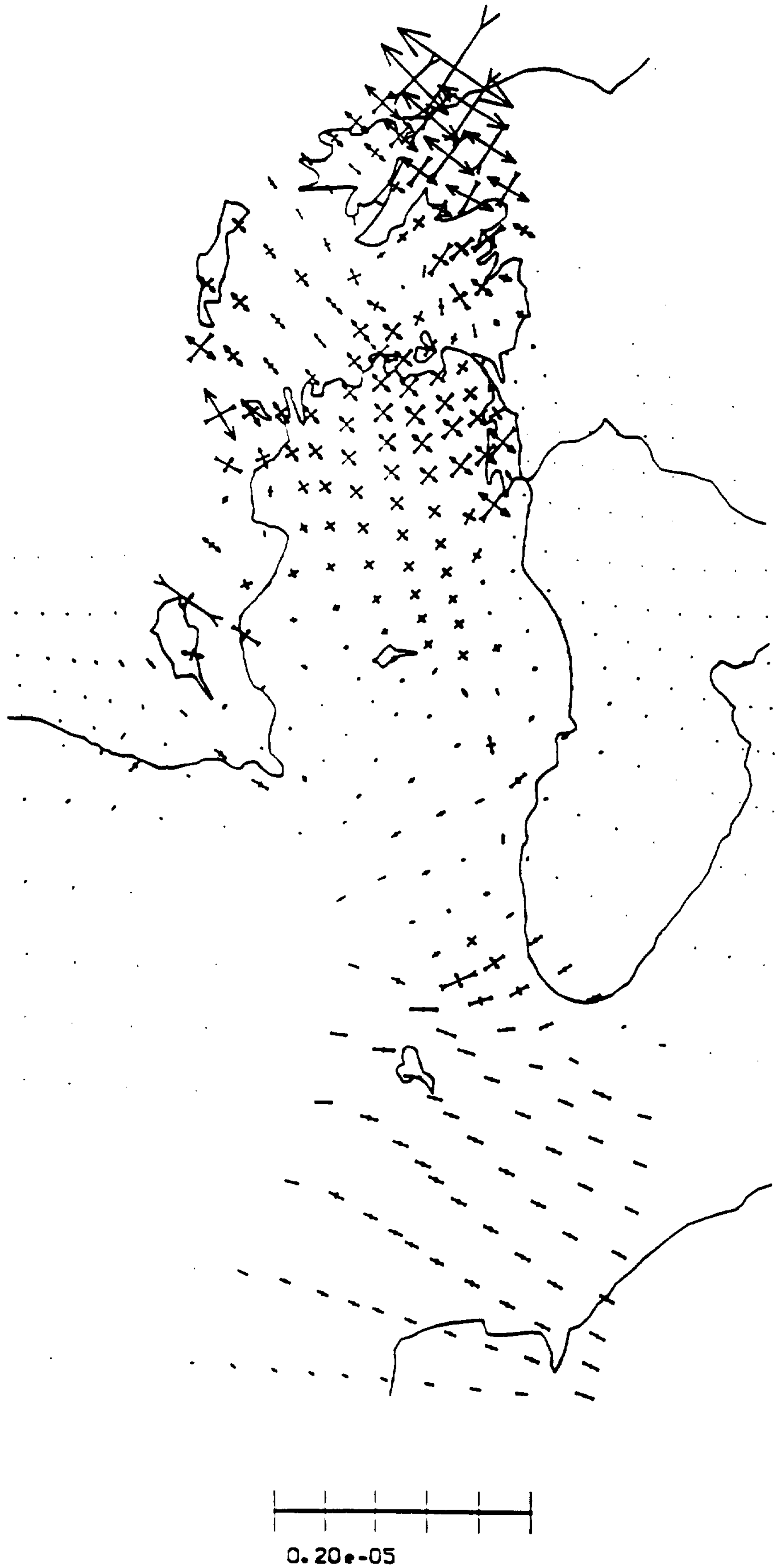

FIG 5c